



# Secondary electron emission model for photo-emission from metals in the vacuum ultraviolet

Ai-Gen Xie<sup>1,2,3</sup> · Yi-Fan Liu<sup>1</sup> · Hong-Jie Dong<sup>1</sup>

Received: 7 May 2022 / Revised: 5 July 2022 / Accepted: 10 July 2022 / Published online: 22 August 2022

© The Author(s), under exclusive licence to China Science Publishing & Media Ltd. (Science Press), Shanghai Institute of Applied Physics, the Chinese Academy of Sciences, Chinese Nuclear Society 2022

**Abstract** This study investigates two secondary electron emission (SEE) models for photoelectric energy distribution curves  $f(E_{\text{ph}}, h\gamma)$ ,  $B$ ,  $E_{\text{mean}}$ , absolute quantum efficiency ( $AQE$ ), and the mean escape depth of photo-emitted electrons  $\lambda$  of metals. The proposed models are developed from the density of states and the theories of photo-emission in the vacuum ultraviolet and SEE, where  $B$  is the mean probability that an internal photo-emitted electron escapes into vacuum upon reaching the emission surface of the metal, and  $E_{\text{mean}}$  is the mean energy of photo-emitted electrons measured from vacuum. The formulas for  $f(E_{\text{ph}}, h\gamma)$ ,  $B$ ,  $\lambda$ ,  $E_{\text{mean}}$ , and  $AQE$  that were obtained were shown to be correct for the cases of Au at  $h\gamma = 8.1\text{--}11.6$  eV, Ni at  $h\gamma = 9.2\text{--}11.6$  eV, and Cu at  $h\gamma = 7.7\text{--}11.6$  eV. The photoelectric cross sections (PCS) calculated here are analyzed, and it was confirmed that the calculated PCS of the electrons in the conduction band of Au at  $h\gamma = 8.1\text{--}11.6$  eV, Ni at  $h\gamma = 9.2\text{--}11.6$  eV, and Cu at  $h\gamma = 7.7\text{--}11.6$  eV are correct.

**Keywords** Absolute quantum efficiency · Photoelectric cross section · Mean escape depth of photo-emitted electrons · Probability · Photo-emission from metals · Secondary electron emission · Vacuum ultraviolet · Mean energy of photo-emitted electrons

## 1 Introduction

The photoelectric effect is important in various domains, such as astrophysics, material analysis applications, photon science, interactions between photons and materials, photo-multipliers, photo-injectors such as RF photo-cathode gun in accelerators, and X-ray sources [1–3]. Photoelectric energy distribution curves  $f(E_{\text{ph}}, h\gamma)$  can be used to characterize the properties of the photoelectric effect,  $E_{\text{ph}}$  is the energy of  $h\gamma$  photon-induced electrons with  $E$  measured from the bottom of the conduction band of metal,  $E$  is the initial energy of electrons measured from the bottom of the conduction band of metal,  $h$  is the Planck constant, and  $\gamma$  is the photon frequency. Thus, many researchers have investigated  $f(E_{\text{ph}}, h\gamma)$  [4, 5]. From the fact that SEE and photo-emissions have the same escape and transport mechanisms [6, 7] and the characteristics of electron-photon interaction and propagation of photons, two formulas for  $f(E_{\text{ph}}, h\gamma)$  from metals in the vacuum ultraviolet have been obtained. Further, the value of  $f(E_{\text{ph}}, h\gamma)$  obtained from Au at  $h\gamma = 8.1\text{--}11.6$  eV, Ni at  $h\gamma = 9.2\text{--}11.6$  eV, and Cu at  $h\gamma = 7.7\text{--}11.6$  eV have been proven to be true.

The absolute quantum efficiency ( $AQE$ )( $h\gamma$ ) and quantum efficiency ( $QE$ )( $h\gamma$ ) are important parameters that are used to characterize photo-emission ability [8–10]. The mean probability that an internal photo-emitted electron

This work was supported by the National Natural Science Foundation of China (No.11873013).

✉ Ai-Gen Xie  
xagth@126.com

- <sup>1</sup> School of Physics and Optoelectronic Engineering, Nanjing University of Information Science & Technology, Nanjing 210044, China
- <sup>2</sup> Jiangsu Key Laboratory for Optoelectronic Detection of Atmosphere and Ocean, Nanjing University of Information Science & Technology, Nanjing 210044, China
- <sup>3</sup> Jiangsu International Joint Laboratory on Meteorological Photonics and Optoelectronic Detection, Nanjing University of Information Science & Technology, Nanjing 210044, China

escapes into vacuum upon reaching the emission surface of metal  $B$  and  $\lambda$  is important parameter of  $AQE(h\gamma)$  and  $QE(h\gamma)$ , where  $\lambda$  denotes the mean escape depth of photo-emitted electrons. The  $B$  is inaccessible to measure; further, the formula for  $B$  and  $\lambda$  has not yet been deduced. It is difficult to measure  $\lambda$ , and the relative differences among the  $\lambda$  values measured by different authors can reach about 100% or more [11–13]. Thus, there is the need for theoretical studies of  $B$  and  $\lambda$ . The value of the mean energy of photo-emitted electrons  $E_{\text{mean}}$  measured from vacuum is an important parameter to assess the mechanisms of energy loss of internal photo-emitted electrons. The internal photo-emitted electrons lose energy mainly by electron–phonon scattering for the case of  $E_{\text{mean}} < 1.0$  eV; however, they lose energy mainly by electron–electron scattering [13] for the case of  $E_{\text{mean}} > 1.0$  eV. From the two formulas for  $f(E_{\text{ph}}, h\gamma)$  deduced here and the definitions of  $B$ ,  $E_{\text{mean}}$ , and  $\lambda$ , the respective formulas for  $B$ ,  $\lambda$ , and  $E_{\text{mean}}$  for metals in the vacuum ultraviolet have been deduced. Based on the fact that the deduced formulas for  $f(E_{\text{ph}}, h\gamma)$  obtained from Au, Ni, and Cu have been experimentally proven and the courses of deducing the formulas for  $B$ ,  $E_{\text{mean}}$ , and  $\lambda$  from metals, it can be concluded that  $B$ ,  $E_{\text{mean}}$ , and  $\lambda$  from Au at  $h\gamma = 8.1$ – $11.6$  eV, Ni at  $h\gamma = 9.2$ – $11.6$  eV, and Cu at  $h\gamma = 7.7$ – $11.6$  eV calculated with corresponding deduced formulas are correct.

Photoelectric cross section PCS is an important topic [14–16], and it has been investigated by many researchers PCS [17]. However, owing to the complexity and difficulty of researching PCS at  $h\gamma < 50$  eV, there are few reported values of measured and calculated PCS at  $h\gamma < 50$  eV [18]. Furthermore, the relative differences among the PCS values at  $h\gamma < 50$  eV obtained by different authors can reach about 200% or more [19]. Thus, it is important to present accurate methods of determining PCS at  $h\gamma < 50$  eV. From the energy band structures of metals, the definition of  $AQE(h\gamma)$ , and one of the formulas for  $f(E_{\text{ph}}, h\gamma)$  deduced here, the formula for  $AQE(h\gamma)$  from metals in the vacuum ultraviolet as a function of the density of states, PCS,  $A_\alpha$ ,  $\Phi$ ,  $E_F$ ,  $E_{\text{ph}}$ ,  $h\gamma$ ,  $s$  and  $\rho$  has been deduced, where  $A_\alpha$  is the molar mass of an atom,  $\rho$  is the material density,  $\Phi$  is the work function,  $E_F$  is the distance from the bottom of conduction band to Fermi level, and  $s$  denotes the number of electrons of conduction band that is provided by one atom. Using the deduced formula for  $AQE(h\gamma)$ , experimental  $AQE(h\gamma)$  [20, 21], and known parameters such as density of states,  $A_\alpha$ ,  $\Phi$ ,  $E_F$ ,  $h\gamma$ ,  $s$ , and  $\rho$ , the PCS of the electrons in the conduction band of Au at  $h\gamma = 8.1$ – $11.6$  eV and Ni at  $h\gamma = 9.2$ – $11.6$  eV are calculated. These calculated PCS are analyzed, and it can be concluded that the calculated PCS of the electrons in the conduction band of Au at  $h\gamma = 8.1$ – $11.6$  eV and Ni at  $h\gamma = 9.2$ – $11.6$  eV are correct, and

that the method presented here of calculating PCS with the deduced formula for  $AQE(h\gamma)$  is a very accurate method.

According to the simple theories of SEE, the fact that SEE and photo-emission have common escape and transport mechanisms [6, 7], and the definition of  $AQE(h\gamma)$ , the universal formula for  $AQE(h\gamma)$  has also been deduced. For negative electron affinity semiconductors (NEAS), the deduced universal formula for  $AQE(h\gamma)$  has the same expression as the existing formula for  $AQE(h\gamma)$  obtained from NEAS used in some studies [22–24]. The method of calculating PCS using the deduced universal formula for  $AQE(h\gamma)$  as well as parameters such as experimental  $AQE(h\gamma)$  [20, 21, 25],  $B$ , and  $\lambda$  is also presented. The PCS of the electrons in the conduction band of Au, Ni, and Cu are calculated using this method and are analyzed. It can be concluded that the calculated PCS of the electrons in the conduction band of Au at  $h\gamma = 8.1$ – $11.6$  eV, Ni at  $h\gamma = 9.2$ – $11.6$  eV, and Cu at  $h\gamma = 7.7$ – $11.6$  eV are correct, and that the proposed method of calculating PCS using the deduced universal formula for  $AQE(h\gamma)$  is more accurate.

## 2 Processes of photo-emission

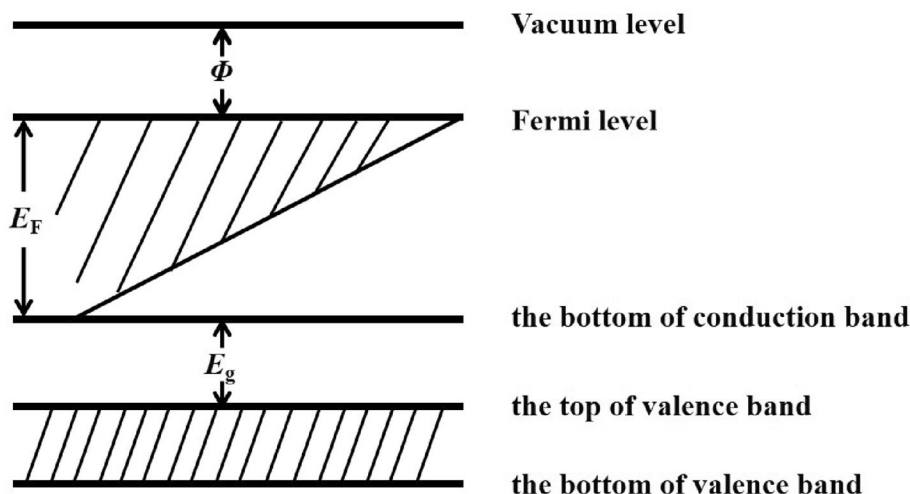
When  $N_0$  photons at  $\gamma < (E_F + E_g)/h$  enter perpendicularly into metals, the number of incident photons at  $x$  can be written as follows [13, 26, 27]:

$$N(x) = N_0 e^{-\alpha_\gamma x} = N_0 e^{-x/\lambda_\gamma}, \quad (1)$$

where  $x$  is the distance from the incident surface to the position at which the photons arrive,  $N_0$  is the number of incident photons at  $x = 0$ , and  $\alpha_\gamma$  is the optical absorption coefficient at  $\gamma$ . From the energy band structures of metals shown in Fig. 1 ( $E_g$  is the distance from the top of the valence band to the bottom of the conduction band of metals), the quantum theory, and law of energy conservation, it is known that in the case that  $N_0$  photons at  $\gamma < (E_F + E_g)/h$  enter perpendicularly into metals, only the electrons in the conduction band of the metal can be excited by the photons.

According to the characteristics of electron-photon interaction, it is known that the probability that all of the electrons in the same energy band of a given metal absorb one photon at a given  $\gamma$  can be approximated as a constant [14, 28, 29]. Thus, the probability that the electron in the conduction band of a given metal absorbs one photon at a given  $\gamma$  can be approximated as a constant  $C_\gamma$ . That is, the PCS at a given  $\gamma$  of the electrons in the conduction band of a given metal can be approximated as a constant  $C_\gamma$ . Based on the energy band structures of metal shown in Fig. 1, the calculated number of electrons per atom per eV  $g(E)$  [20, 21, 25], the values of  $E_F$ , the law of energy

**Fig. 1** Schematic energy band structures of metals



conservation, and the fact that  $\gamma$  is  $< (E_F + E_g)/h$ , we can calculate the relative number of electrons in the conduction band of a metal that may absorb one photon and become photo-excited electrons. For example, when the photons at  $h\gamma = 7.4$  eV enter Au with  $E_F = 11.6$  eV [20], the electrons with  $E \geq (E_F - 7.4$  eV) (*i.e.*, 4.2 eV) may absorb one photon and become photo-excited electrons. Thus, based on the  $g(E)$  value of Au [20], the fact that the electrons with  $E \geq 4.2$  eV may become photo-excited electrons and the fact that the  $E_F$  value of Au equals 11.6 eV, we can obtain  $n\%$  of electrons in the conduction band of Au, which may absorb one photon and become photo-excited electrons based on calculations, and the obtained  $n\%$  for Au at  $h\gamma = 7.4$  eV equals 0.808; using the same method, we obtain  $n\%$  at different  $h\gamma$  values of Au, Ni, and Cu, and the corresponding results are shown in Tables 1, 2, and 5, respectively. Therefore, from the definition of  $\alpha_\gamma$  [13, 26] in

Eq. (1) and the fact that the probability that the electron in the conduction band of a given metal absorbs one photon at a given  $\gamma$  can be considered as a constant  $C_\gamma$ , the  $\alpha_\gamma$  parameter of Eq. (1) can be written as

$$\alpha_\gamma = (\lambda_\gamma)^{-1} = (s\rho C_\gamma n\% N_A) / A_x. \tag{2}$$

The unit of  $\rho$  is  $\text{g/m}^3$ , the unit of  $A_x$  is  $\text{g/mol}$ , and  $N_A$  denotes the Avogadro constant.

Based on the fact that  $E_{\text{ph}}$  is the energy of  $h\gamma$  photon-induced electrons with  $E$  measured from the bottom of the conduction band of a metal, the relation  $E = E_{\text{ph}}h\gamma$  is obtained. Some authors have calculated  $g(E)$  [20, 21, 25] and the energy distribution of electrons in the conduction band of metal with  $V = 1.0 \text{ m}^3 G(E)$  (*i.e.*, density of states of conduction band of metal) [30, 31]. According to the definitions of  $G(E)$  and  $g(E)$  and the relation  $E = E_{\text{ph}}h\gamma$ , the

**Table 1** The parameters of Au calculated using the first SEE model

$h\gamma(\text{eV})$	Experimental $AQE(h\gamma)$ [20]	Calculated $AQE(h\gamma)$	$m\%$ [20]	$n\%$ [20]	$C_\gamma$ ( $10^{-23} \text{ m}^2$ )	$\lambda_\gamma$ ( $10^{-9} \text{ m}$ )	$\lambda$ ( $10^{-9} \text{ m}$ )	$B$	$E_{\text{mean}}$ (eV)
7.4	0.000800	0.000696	0.0734	0.808	34.3	5.56	2.590	0.0241	1.38
7.7	0.00110	0.000975	0.106	0.845	35.2	5.18	2.56	0.0235	1.46
7.9	0.00140	0.00125	0.135	0.867	37.0	4.81	2.56	0.0231	1.49
8.1	0.00175	0.00158	0.167	0.887	37.8	4.60	2.55	0.0235	1.52
8.7	0.00320	0.00297	0.266	0.938	40.2	4.09	2.50	0.0276	1.82
9.0	0.00420	0.00392	0.320	0.957	41.9	3.84	2.45	0.0301	1.99
9.2	0.00510	0.00479	0.355	0.968	45.2	3.52	2.42	0.0303	2.07
10.4	0.01000	0.00952	0.506	0.995	45.4	3.41	2.16	0.0483	2.55
10.7	0.01200	0.0114	0.548	0.996	49.8	3.11	2.12	0.0509	2.70
11.0	0.01400	0.0133	0.597	0.998	53.1	2.96	2.04	0.0538	2.85
11.2	0.01520	0.0144	0.631	0.999	53.9	2.86	2.00	0.0553	2.93
11.5	0.01700	0.0161	0.682	0.999	54.5	2.83	1.96	0.0575	3.06

**Table 2** The parameters of Ni calculated using the first SEE model

$h\gamma$ (eV)	Experimental $AQE(h\gamma)$ [21]	Calculated $AQE(h\gamma)$	$n\%$ [21]	$m\%$ [21]	$C_\gamma$ ( $10^{-23}$ m <sup>2</sup> )	$\lambda_\gamma$ ( $10^{-9}$ m)	$\lambda$ ( $10^{-9}$ m)	$B$	$E_{\text{mean}}$ (eV)
7.6	$3.00 \times 10^{-3}$	$2.67 \times 10^{-3}$	1.00	0.362	10.4	10.5	1.74	0.0520	1.83
8.0	$5.17 \times 10^{-3}$	$4.45 \times 10^{-3}$	1.00	0.415	14.8	7.40	1.67	0.0583	2.05
8.6	$7.82 \times 10^{-3}$	$6.70 \times 10^{-3}$	1.00	0.496	17.6	6.22	1.58	0.0667	2.39
9.2	$1.15 \times 10^{-2}$	$9.78 \times 10^{-2}$	1.00	0.605	21.3	5.14	1.51	0.0712	2.71
9.8	$1.52 \times 10^{-2}$	$1.27 \times 10^{-2}$	1.00	0.766	22.7	4.83	1.46	0.0712	2.96
10.4	$2.49 \times 10^{-2}$	$2.11 \times 10^{-2}$	1.00	0.921	32.5	3.37	1.43	0.0769	3.18
10.5	$2.81 \times 10^{-2}$	$2.40 \times 10^{-2}$	1.00	0.938	36.8	2.98	1.42	0.0791	3.23
10.6	$2.99 \times 10^{-2}$	$2.70 \times 10^{-2}$	1.00	0.953	41.3	2.65	1.41	0.0815	3.28
10.8	$3.05 \times 10^{-2}$	$2.62 \times 10^{-2}$	1.00	0.978	36.0	3.04	1.39	0.0853	3.35
11.0	$3.14 \times 10^{-2}$	$2.71 \times 10^{-2}$	1.00	1.00	34.6	3.17	1.37	0.0896	3.45
11.2	$3.18 \times 10^{-2}$	$2.78 \times 10^{-2}$	1.00	1.00	32.8	3.34	1.35	0.0965	3.56
11.4	$3.20 \times 10^{-2}$	$2.82 \times 10^{-2}$	1.00	1.00	31.1	3.52	1.33	0.103	3.68
11.6	$3.22 \times 10^{-2}$	$2.87 \times 10^{-2}$	1.00	1.00	29.7	3.69	1.3	0.11	3.81

relation between  $G(E)$  and  $g(E)$  (*i.e.*, the relation  $G(E_{\text{ph}}h\gamma)$  and  $g(E_{\text{ph}}h\gamma)$ ) can be written as [30, 31]

$$G(E) = (\rho N_{\text{A}} g(E)) / A_x = G(E_{\text{ph}} - h\gamma) \\ = (\rho N_{\text{A}} g(E_{\text{ph}} - h\gamma)) / A_x. \quad (3)$$

Processes involved in photo-emission may be considered as three-step processes [21]: first, electrons are excited to become internal photo-emitted electrons; second, a portion of the internal photo-emitted electrons propagate to the emission surface; and third, a portion of the internal photo-emitted electrons reaching the emission surface escape into the vacuum and become photo-emitted electrons. The three-step processes of photo-emission from metal which are investigated in detail in this work are as follows:

Owing to the fact that the PCS for a given  $\gamma$  value of the electrons in the conduction band of a given metal can be considered as a constant  $C_\gamma$ , definitions of  $\alpha_{\text{ph}\gamma}$ ,  $G(E_{\text{ph}}h\gamma)$ , and  $g(E_{\text{ph}}h\gamma)$  [13, 26, 30, 31] and Eqs. (1) and (3), in the case that  $N$  photons at  $\gamma < (E_{\text{F}} + E_{\text{g}})/h$  enter perpendicularly into metals, the number of internal photo-emitted electrons at  $x$  per unit path length of incident photons can be written as:

$$n(x) = \alpha_{\text{ph}\gamma} N(x) = C_\gamma G(E_{\text{ph}} - h\gamma) N(x) = C_\gamma G(E_{\text{ph}} - h\gamma) N_0 e^{-\alpha_\gamma x} \\ = \frac{C_\gamma \rho N_{\text{A}} g(E_{\text{ph}} - h\gamma) N_0 e^{-x/\lambda_\gamma}}{A_x} [(E_{\text{ph}} - \Phi - E_{\text{F}}) \geq 0], \quad (4)$$

where  $\alpha_{\text{ph}\gamma}$  is the photoelectric absorption coefficient at  $\gamma$ .

Most secondary electrons have energy  $E_{\text{vac}} > 1.0$  eV [32, 33], and the mean energy of secondary electrons emitted from metal  $E_{\text{am}}$  is much larger than 1.0 eV, and both  $E_{\text{vac}}$  and  $E_{\text{am}}$  are measured from vacuum. In the case

that  $E_{\text{am}}$  is much larger than 1.0 eV, the mean escape depth of secondary electrons with  $E_0$  ( $0 \leq (E_0 - \Phi - E_{\text{F}}) \leq 1.5E_{\text{F}}$ ) in metals can be expressed as [34, 35]

$$\lambda(E_0, \text{metal}) = \frac{2.0 \times 10^{-8}}{(E_0 - E_{\text{F}})^{1.3}} \left( \frac{E_{\text{F}}}{5.57} \right)^{0.45} \\ [0 \leq (E_0 - \Phi - E_{\text{F}}) \leq 1.5E_{\text{F}}], \quad (5)$$

where  $E_0$  is measured from the bottom of the conduction band, and  $E_0$  is the sum of  $E$  and the energy obtained from primary electrons by scattering. The unit of length in this study is m, but the unit of length in Refs. [34, 35] is Å. Therefore, in this study, the magnitude of the formula coefficient in Refs. [34, 35] is  $10^{10}$  times that in Eq. (5).

According to the energy band structures of metals, the fact that the electrons with  $E$  absorbing one  $h\gamma$  photon have  $(E + h\gamma)$  (*i.e.*,  $E_{\text{ph}}$ ) and the theories of photo-emission, we estimate that in the case that  $\gamma$  is farther away  $\gamma_0$  { *i.e.*,  $\gamma > [(3.0 \text{ eV}/h) + \gamma_0]$ }, most of the  $h\gamma$  photon-induced electrons in metals have  $E_{\text{vac}} > 1.0$  eV, and  $E_{\text{mean}}$  is much larger than 1.0 eV, where  $\gamma_0$  is the threshold frequency. Thus, from the fact that SEE and photo-emission have common escape and transport mechanisms [6, 7] and the fact that most secondary electrons in metals also have  $E_{\text{vac}} > 1.0$  eV and  $E_{\text{am}}$  is also much larger than 1.0 eV, it is known that the  $h\gamma$  photon-induced electrons with  $E_{\text{ph}}$  that undergo photo-emission from metals farther than  $\gamma_0$  have the same transport mechanisms as do secondary electrons in metals. Further, the mean escape depth of  $h\gamma$  photon-induced electrons with  $E_{\text{ph}}$  that undergo photo-emission from metals farther away than  $\gamma_0$   $\lambda(E_{\text{ph}}, h\gamma)$  has a similar expression as does Eq. (5). Therefore, according to Eq. (5) and the fact that the electrons with  $E$  absorbing one  $h\gamma$  photon have an  $E_{\text{ph}}$  value that corresponds to  $E_0$ , in the case where  $E_{\text{mean}}$  is much larger than 1.0 eV,  $\lambda(E_{\text{ph}}, h\gamma)$  can be written as

$$\begin{aligned} \lambda(E_{\text{ph}}, h\gamma) &= \frac{2.0 \times 10^{-8}}{(E + h\gamma - E_F)^{1.3}} \left(\frac{E_F}{5.57}\right)^{0.45} \\ &= \frac{2.0 \times 10^{-8}}{(E_{\text{ph}} - E_F)^{1.3}} \left(\frac{E_F}{5.57}\right)^{0.45} \quad [0 \leq (E_{\text{ph}} - \Phi - E_F) \leq 1.5E_F] \end{aligned} \tag{6}$$

The probability that an internal secondary electron having  $E_0 \geq (\Phi + E_F)$  and reaching an emission surface passes over the surface barrier of a metal into a vacuum [34–36] is expressed as

$$P(E_0) = 1 - [(E_F + \Phi)/E_0]^{0.5}. \tag{7}$$

From Eq. (7), the fact that photo-emission and SEE have common escape mechanisms [6, 7] and the fact that  $E_0$  corresponds to  $E_{\text{ph}} = E + h\gamma$ , the probability that an internal photo-emitted electron with  $E$  absorbing one  $h\gamma$  photon, having  $E_{\text{ph}} \geq (\Phi + E_F)$  and reaching an emission surface passes over the surface barrier of metal can be written as [36, 37]

$$\begin{aligned} P(E_{\text{ph}}, h\gamma) &= 1 - [(E_F + \Phi)/(E + h\gamma)]^{0.5} \\ &= 1 - [(E_F + \Phi)/E_{\text{ph}}]^{0.5}. \end{aligned} \tag{8}$$

Based on Eqs. (6) and (8), the probability that an internal photo-emitted electron with  $E$ , which absorbs one  $h\gamma$  photon and is excited at  $x$ , can reach an emission surface and pass over the surface can be written as

$$P(E_{\text{ph}}, h\gamma, x) = \left\{1 - [(E_F + \Phi)/E_{\text{ph}}]^{0.5}\right\} e^{-\frac{x}{\lambda(E_{\text{ph}}, h\gamma)}}. \tag{9}$$

### 3 First SEE model for photo-emission

Based on the fact that SEE has a maximum escape depth that is five times the mean escape depth [34, 35, 37], it is easy to understand that this is also applicable for photo-emitted electrons because both of them have common escape and transport mechanisms [6, 7]. Thus,  $f(E_{\text{ph}}, h\gamma)$  can be given as

$$\begin{aligned} f(E_{\text{ph}}, h\gamma) &= \int_0^\infty (n(x)P(E_{\text{ph}}, h\gamma, x))dx \\ &= \int_0^{5\lambda(E_{\text{ph}}, h\gamma)} \left\{n(x)e^{-\frac{x}{\lambda(E_{\text{ph}}, h\gamma)}} \left[1 - \left(\frac{E_F + \Phi}{E_{\text{ph}}}\right)^{0.5}\right]\right\} dx \\ &= \frac{C_\gamma \rho N_A g(E_{\text{ph}} - h\gamma) N_0 \lambda_{\text{real}}}{A_x} \left(1 - e^{-\frac{5\lambda(E_{\text{ph}}, h\gamma)}{\lambda_{\text{real}}}}\right) \left[1 - \left(\frac{E_F + \Phi}{E_{\text{ph}}}\right)^{0.5}\right] \end{aligned} \tag{10}$$

where  $\lambda_{\text{real}}$  of Eq. (10) can be written as

$$\lambda_{\text{real}} = \lambda(E_{\text{ph}}, h\gamma) \lambda_\gamma / (\lambda(E_{\text{ph}}, h\gamma) + \lambda_\gamma). \tag{11}$$

Based on the energy band structures of metals shown in Fig. 1, Eq. (8), and the fact that the electrons with  $E$  absorbing one  $h\gamma$  photon have  $E_{\text{ph}} = (E + h\gamma)$ , it is known that in the case that  $N_0$  photons at  $\gamma < (E_F + E_g)/h$  enter into metals, the electrons with  $E$  in the range of  $[(E_F + \Phi - h\gamma), (E_F + \Phi)]$  absorbing one  $h\gamma$  photon have  $E_{\text{ph}}$  in the range of  $[(E_F + \Phi), (E_F + \Phi + h\gamma)]$ , and that the photo-emitted electrons with  $E_{\text{ph}}$  in the range of  $[(E_F + \Phi), (E_F + \Phi + h\gamma)]$  may escape into the vacuum. Thus, from Eq. (10), it is known that in the case that  $N$  photons at  $\gamma < (E_F + E_g)/h$  enter perpendicularly into metals, the number of photo-emitted electrons can be written as

$$\begin{aligned} N_{\text{electrons}} &= \frac{C_\gamma \rho N_A}{A_x} \int_{(E_F + \Phi)}^{(E_F + \Phi + h\gamma)} \left\{N_0 g(E_{\text{ph}} - h\gamma) \lambda_{\text{real}} \right. \\ &\quad \left. \left(1 - e^{-\frac{5\lambda(E_{\text{ph}}, h\gamma)}{\lambda_{\text{real}}}}\right) \left[1 - \left(\frac{E_F + \Phi}{E_{\text{ph}}}\right)^{0.5}\right]\right\} dE_{\text{ph}}. \end{aligned} \tag{12}$$

$AQE(h\gamma)$  is defined as the number of photo-emitted electrons per absorbed photon [38, 39]. Thus, from the definition of  $AQE(h\gamma)$ , the fact that  $N_0$  photons at  $\gamma < (E_F + E_g)/h$  are absorbed by metals and Eq. (12), the  $AQE(h\gamma)$  from metals induced by photons at  $\gamma < (E_F + E_g)/h$  can be written as

$$\begin{aligned} AQE(h\gamma) &= \frac{C_\gamma \rho N_A}{A_x} \int_{(E_F + \Phi)}^{(E_F + \Phi + h\gamma)} \left\{g(E_{\text{ph}} - h\gamma) \lambda_{\text{real}} \right. \\ &\quad \left. \left(1 - e^{-\frac{5\lambda(E_{\text{ph}}, h\gamma)}{\lambda_{\text{real}}}}\right) \left[1 - \left(\frac{E_F + \Phi}{E_{\text{ph}}}\right)^{0.5}\right]\right\} dE_{\text{ph}}. \end{aligned} \tag{13}$$

From Ref. [20], it is known that the  $g(E)$  (*i.e.*,  $g(E_{\text{ph}}, h\gamma)$ ) of Au is as shown in Fig. 1 of Ref. 20, and that the  $s$ ,  $E_F$ , and  $\Phi$  values of Au equal 11, 11.6 eV, and 4.9 eV, respectively. The  $C_\gamma$  value of Au calculated with parameters ( $h\gamma$ ,  $N_A$ ,  $s$ ,  $\rho = 1.93 \times 10^7$  g/m<sup>3</sup>,  $A_x = 197$  g/mol [40],  $g(E_{\text{ph}}, h\gamma)$  [20],  $E_F$ ,  $\Phi$ ,  $n\%$  and experimental  $AQE(h\gamma)$  [20] shown in Table 1) and Eqs. (2), (6), (11), and (13) are still shown in Table 1. The  $\lambda_\gamma$  value of Au calculated using Eq. (2) and parameters ( $s$ ,  $N_A$ ,  $\rho$ ,  $A_x$ ,  $n\%$ , and  $C_\gamma$  shown in Table 1) are also shown in Table 1. The values of  $f(E_{\text{ph}}, h\gamma)$  (in arbitrary units) of Au are calculated with parameters ( $E_{\text{ph}}$ ,  $h\gamma$ ,  $g(E_{\text{ph}}, h\gamma)$ ,  $E_F$ ,  $\Phi$ ,  $\lambda_\gamma$ , and  $C_\gamma$ , as shown in Table 1) and Eqs. (6), (10), and (11). The comparison between these calculated  $f(E_{\text{ph}}, h\gamma)$  values of Au and the experimental ones [20] is shown in Fig. 2.

From Ref. [21], it is known that the  $g(E_{\text{ph}}, h\gamma)$  value of Ni is as shown in Fig. 18 of Ref. [21], and that the  $s$ ,  $E_F$ , and  $\Phi$  values of Ni equal 10, 6.0 eV, and 5.0 eV, respectively. The  $C_\gamma$  at  $h\gamma \leq 11.0$  eV of Ni calculated with parameters ( $h\gamma$ ,  $N_A$ ,  $s$ ,

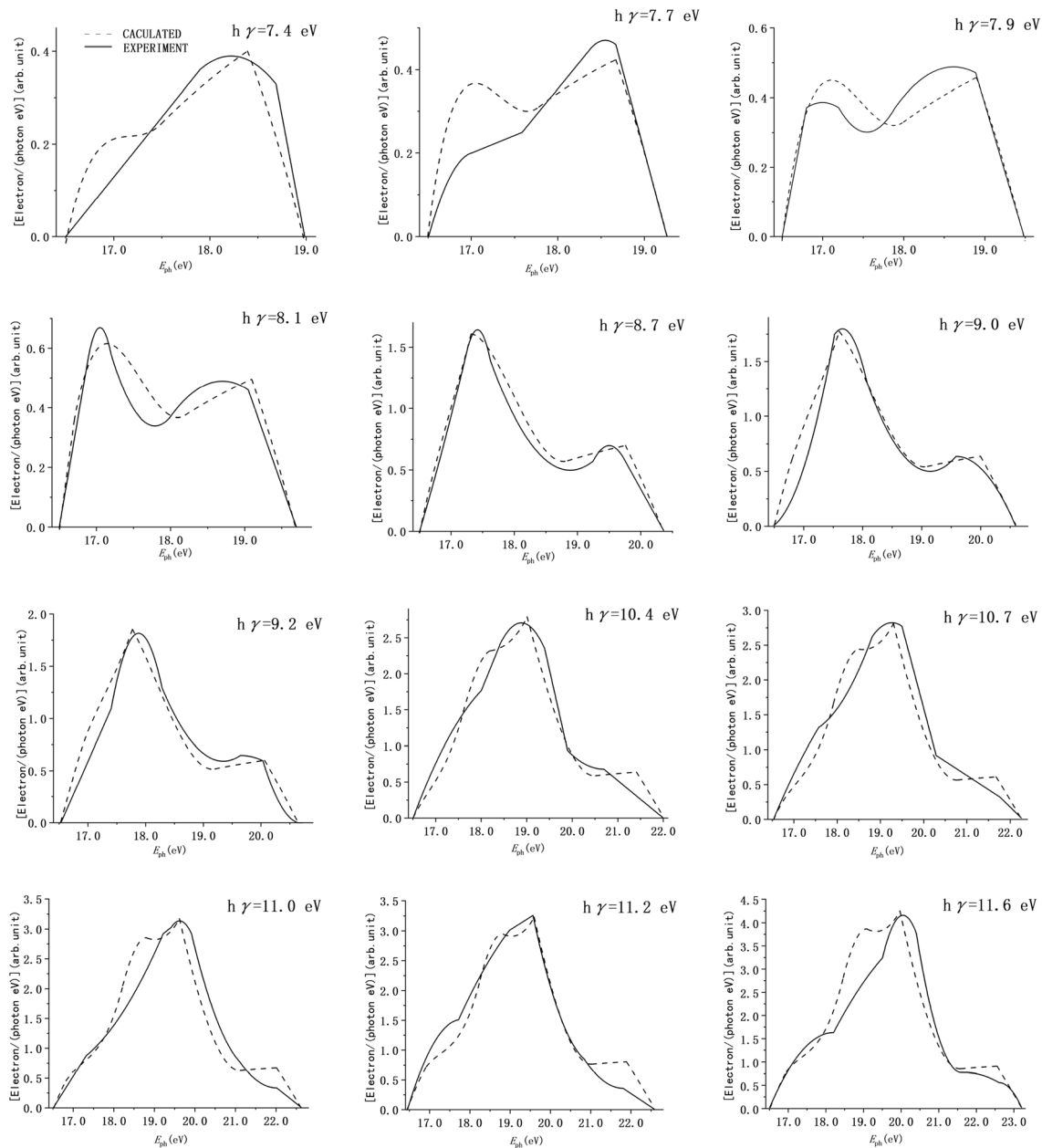


**Fig. 2** Comparison between the  $f(E_{ph}, h\gamma)$  values of Au calculated using Eq. (10) and experimentally obtained values

$\rho = 8.9 \times 10^6 \text{ g/m}^3$ ,  $A_\alpha = 58.69 \text{ g/mol}$  [40],  $g(E_{ph}h\gamma)$  [21],  $E_F$ ,  $\Phi$ ,  $n\%$ , and  $AQE(h\gamma)$  [21] shown in Table 2) and Eqs. (2), (6), (11), and (13) are as shown in Table 2. The sum of  $E_F$  and  $\Phi$  of Ni is equal to 11.0 eV. Thus, from Fig. 1, when we use parameters ( $h\gamma$ ,  $N_A$ ,  $s$ ,  $\rho$ ,  $A_\alpha$ ,  $g(E_{ph}h\gamma)$ ,  $E_F$ ,  $\Phi$ ,  $n\%$ , and experimental  $AQE(h\gamma)$  [21] shown in Table 2) and Eqs. (2), (6), (11), and (13) to calculate the value of  $C_\gamma$  at  $h\gamma > 11.0 \text{ eV}$  for Ni, the lower limit of the integral [*i.e.*,  $(E_F + \Phi)$ ] in Eq. (13) should be replaced with “ $h\gamma$ ”. The  $\lambda_\gamma$  of Ni calculated with Eq. (2) and parameters ( $s$ ,  $N_A$ ,  $\rho$ ,  $A_\alpha$ ,  $n\%$ , and  $C_\gamma$  shown in Table 2) are also shown in Table 2. The  $f(E_{ph}, h\gamma)$  value (in arbitrary units) of Ni calculated with corresponding parameters ( $E_{ph}$ ,  $h\gamma$ ,

$g(E_{ph}h\gamma)$ ,  $E_F$ ,  $\Phi$ ,  $\lambda_\gamma$ , and  $C_\gamma$  shown in Table 2) and Eqs. (6), (10), and (11) are shown in Fig. 3.

Based on Eq. (12) and three-step processes of photo-emission, it is known that in the case where  $N_0$  photons at  $\gamma < (E_F + E_g)/h$  enter perpendicularly into metals, the number of internal photo-emitted electrons reaching the surface can be written as

$$N_{\text{reach}} = \frac{C_\gamma \rho N_A}{A_\alpha} \int_{(E_F + \Phi)}^{(E_F + \Phi + h\gamma)} \left[ N_0 g(E_{ph} - h\gamma) \lambda_{\text{real}} \left( 1 - e^{-\frac{S(E_{ph}h\gamma)}{\lambda_{\text{real}}}} \right) \right] dE_{ph}. \tag{14}$$

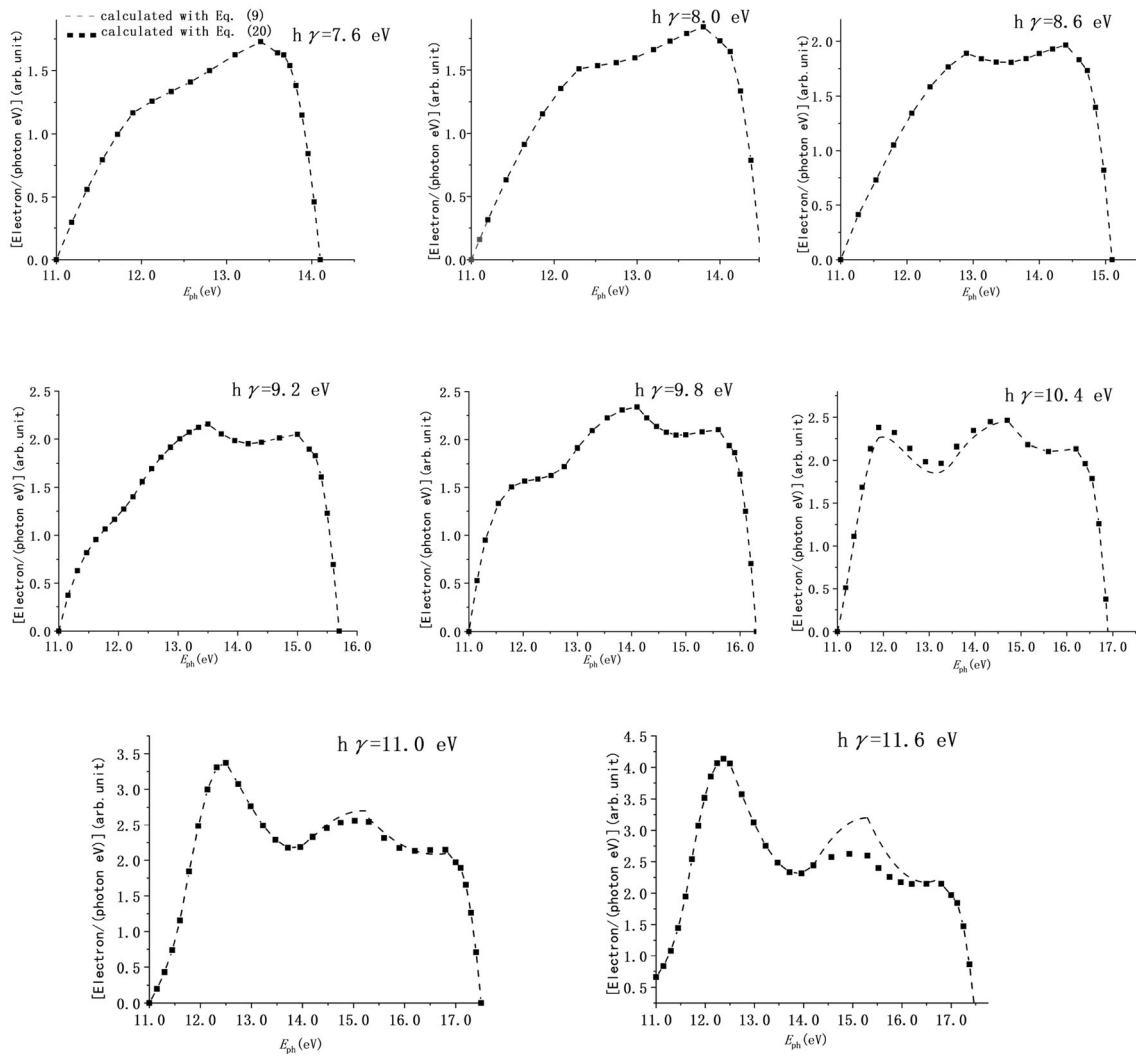


**Fig. 3** The  $f(E_{ph}, h\gamma)$  values calculated using Eqs. (10) and Eq. (21) for Ni

Based on Eqs. (6) and (12), it is known that in the case that  $N_0$  photons at  $\gamma < (E_F + E_g)/h$  enter perpendicularly into metals, the total escape depth of photo-emitted electrons can be written as

$$N_{\text{depth}} = \frac{C_\gamma \rho N_A}{A_z} \int_{(EF+\Phi)}^{(EF+\Phi+h\gamma)} \left\{ N_0 g(E_{\text{ph}} - h\gamma) \lambda(E_{\text{ph}}, h\gamma) \lambda_{\text{real}} \left( 1 - e^{-\frac{5\lambda(E_{\text{ph}}h\gamma)}{\lambda_{\text{real}}}} \right) \left[ 1 - \left( \frac{E_F + \Phi}{E_{\text{ph}}} \right)^{0.5} \right] \right\} dE_{\text{ph}} \tag{15}$$

According to Eq. (12) and the fact that the photo-emitted electrons with  $E$  absorbing one  $h\gamma$  photon have  $E_{\text{vac}} = (E_{\text{ph}} - E_F - \Phi)$ , it is known that in the case that  $N_0$  photons at  $\gamma < (E_F + E_g)/h$  enter perpendicularly into metals, the total  $E_{\text{vac}}$  of photo-emitted electrons can be written as

$$N_{\text{energy}} = \frac{C_\gamma \rho N_A}{A_z} \int_{(EF+\Phi)}^{(EF+\Phi+h\gamma)} \left\{ N_0 g(E_{\text{ph}} - h\gamma) (E_{\text{ph}} - E_F - \Phi) \lambda_{\text{real}} \left( 1 - e^{-\frac{5\lambda(E_{\text{ph}}h\gamma)}{\lambda_{\text{real}}}} \right) \left[ 1 - \left( \frac{E_F + \Phi}{E_{\text{ph}}} \right)^{0.5} \right] \right\} dE_{\text{ph}} \tag{16}$$

Based on the definition of  $B$  and Eqs. (12) and (14),  $B$  can be expressed as

$$B = N_{\text{electrons}} / N_{\text{reach}} \tag{17}$$

From the definition of  $\lambda$  and Eqs. (12) and (15),  $\lambda$  can be written as

$$\lambda = N_{\text{depth}} / N_{\text{electrons}} \tag{18}$$

Based on the definition of  $\lambda$  and Eqs. (12) and (16),  $E_{\text{mean}}$  can be expressed as

$$E_{\text{mean}} = N_{\text{energy}}/N_{\text{electrons}}. \tag{19}$$

The  $B$  values of Au and Ni are calculated using Eqs. (6), (11), (12), (14), and (17) and corresponding parameters ( $h\gamma$ ,  $g(E_{\text{ph}}h\gamma)$ ,  $E_{\text{F}}$ ,  $\Phi$ ,  $\lambda_{\gamma}$  shown in Tables 1, 2), respectively; The  $\lambda$  values of Au and Ni are calculated using Eqs. (6), (11), (12), (15), and (18) and corresponding parameters ( $h\gamma$ ,  $g(E_{\text{ph}}h\gamma)$ ,  $E_{\text{F}}$ ,  $\Phi$ ,  $\lambda_{\gamma}$  shown in Tables 1 and 2). The  $E_{\text{mean}}$  values of Au and Ni are calculated using Eqs. (6), (11), (12), (16), and (19), and corresponding parameters ( $h\gamma$ ,  $g(E_{\text{ph}}h\gamma)$ ,  $E_{\text{F}}$ ,  $\Phi$ ,  $\lambda_{\gamma}$  shown in Tables 1 and 2). These calculated  $B$ ,  $\lambda$ , and  $E_{\text{mean}}$  values of Au and Ni are shown in Tables 1 and 2.

The sum of the  $E_{\text{F}}$  and  $\Phi$  values of Ni is equal to 11.0 eV [21]. Thus, in the case that photons at  $h\gamma > 11.0$  eV enter Ni, the electrons in the conduction band absorbing one  $h\gamma$  photon at least have  $E_{\text{ph}} = h\gamma$ . Therefore, when we use Eqs. (12) and (14)–(19) to calculate the corresponding parameters ( $B$ ,  $\lambda$  and  $E_{\text{mean}}$ ) at  $h\gamma > 11.0$  eV for Ni, the lower limit of the integral in Eqs. (12) and (14)–(16) should be replaced with “ $h\gamma$ ”. These calculated  $B$ ,  $\lambda$  and  $E_{\text{mean}}$  values of Ni are shown in Table 2.

From the energy band structures of metal shown in Fig. 1, the law of energy conservation, the relation of  $E_{\text{ph}} = E + h\gamma$ , and the courses of deducing Eqs. (12)–(16), it is known that in the case that  $h\gamma$  is within the range of  $((E_{\text{F}} + \Phi), (E_{\text{F}} + E_{\text{g}}))$ , the lower limit of the integral in Eqs. (12)–(16) should be replaced with “ $h\gamma$ ”.

### 4 Second SEE model for photo-emission

From the above courses of calculating  $C_{\gamma}$  with Eqs. (2), (6), (11), and (13), it is known that in the cases that the  $AQE(h\gamma)$  or absolute  $g(E_{\text{ph}}h\gamma)$  values are not known,  $C_{\gamma}$  cannot be calculated using Eqs. (2), (6), (11), and (13). From the above courses of calculating  $\lambda_{\gamma}$ ,  $f(E_{\text{ph}}, h\gamma)$ ,  $B$ ,  $\lambda$  and  $E_{\text{mean}}$ , it is also known that  $\lambda_{\gamma}$ ,  $f(E_{\text{ph}}, h\gamma)$ ,  $B$ ,  $\lambda$ , and  $E_{\text{mean}}$  can be calculated by the first SEE model for photo-emission on the basis of the known  $C_{\gamma}$ . Thus, in the case that  $AQE(h\gamma)$  or the absolute  $g(E_{\text{ph}}h\gamma)$  value is not known,  $\lambda_{\gamma}$ ,  $f(E_{\text{ph}}, h\gamma)$ ,  $B$ ,  $\lambda$ , and  $E_{\text{mean}}$  cannot be calculated by the first SEE model either. Therefore, we present the following second SEE model for  $f(E_{\text{ph}}, h\gamma)$ ,  $C_{\gamma}$ ,  $\lambda_{\gamma}$ ,  $B$ ,  $\lambda$ , and  $E_{\text{mean}}$  of metals; in the case that both  $AQE(h\gamma)$  and the absolute  $g(E_{\text{ph}}h\gamma)$  values are not known,  $f(E_{\text{ph}}, h\gamma)$ ,  $B$ ,  $\lambda$ , and  $E_{\text{mean}}$  can still be calculated by the second SEE model. In the case that the absolute  $g(E_{\text{ph}}h\gamma)$  value is not known,  $C_{\gamma}$  and  $\lambda_{\gamma}$  can still be calculated by the second SEE model.

Suppose that in the case that  $N_0$  photons at  $\gamma < (E_{\text{F}} + E_{\text{g}})/h$  enter perpendicularly into metals, the number of photons at  $x$  does not decrease with increasing  $x$ , and equals  $N_0$ . Thus, based on Eq. (3), the above assumption,

and the fact that the PCS at a given  $\gamma$  of the electron in the conduction band of a given metal can be considered as a constant  $C_{\gamma}$ , in the case that  $N_0$  photons at  $\gamma < (E_{\text{F}} + E_{\text{g}})/h$  enter into metals, the number of internal photo-emitted electrons per unit path length of incident photons can be written as

$$n(x) = C_{\gamma}G(E_{\text{ph}} - h\gamma)N_0 = \frac{C_{\gamma}\rho N_{\text{A}}g(E_{\text{ph}} - h\gamma)N_0}{A_x} \quad [0 \leq (E_{\text{ph}} - \Phi - E_{\text{F}})]. \tag{20}$$

Therefore, from the three-step processes of photo-emission, the conclusion that the maximum escape depth of internal photo-emitted electrons with  $E_{\text{ph}}$  equals  $5.0 \lambda(E_{\text{ph}}, h\gamma)$  and Eqs. (9) and (20),  $f(E_{\text{ph}}, h\gamma)$  can be expressed as

$$f(E_{\text{ph}}, h\gamma) = \int_0^{5\lambda(E_{\text{ph}}, h\gamma)} \left\{ \frac{C_{\gamma}\rho N_{\text{A}}g(E_{\text{ph}} - h\gamma)N_0}{A_x} e^{-\frac{x}{\lambda(E_{\text{ph}}, h\gamma)}} \left[ 1 - \left( \frac{E_{\text{F}} + \Phi}{E_{\text{ph}}} \right)^{0.5} \right] \right\} dx = \frac{C_{\gamma}\rho N_{\text{A}}g(E_{\text{ph}} - h\gamma)N_0\lambda(E_{\text{ph}}, h\gamma)}{A_x} (1 - e^{-5}) \left[ 1 - \left( \frac{E_{\text{F}} + \Phi}{E_{\text{ph}}} \right)^{0.5} \right] [0 \leq (E_{\text{ph}} - \Phi - E_{\text{F}}) \leq 1.5E_{\text{F}}] \tag{21}$$

The  $f(E_{\text{ph}}, h\gamma)$  (in arbitrary units) values of Au are calculated with corresponding parameters ( $E_{\text{ph}}$ ,  $h\gamma$ ,  $g(E_{\text{ph}}h\gamma)$  [20],  $E_{\text{F}}$ ,  $\Phi$ ) and Eqs. (6) and (21). The comparison between these calculated  $f(E_{\text{ph}}, h\gamma)$  values of Au and experimental ones [20] are shown in Fig. 4. The  $f(E_{\text{ph}}, h\gamma)$  value (in arbitrary units) of Ni calculated using corresponding parameters ( $E_{\text{ph}}$ ,  $h\gamma$ ,  $g(E_{\text{ph}}h\gamma)$  [21],  $E_{\text{F}}$ ,  $\Phi$ ) and Eqs. (6) and (21) are also shown in Fig. 3. From Ref. [25], it is known that the  $g(E_{\text{ph}}h\gamma)$  value (in arbitrary units) of Cu is shown in Fig. 4 of Ref. [25], and that the  $E_{\text{F}}$ ,  $s$ , and  $\Phi$  values of Cu equal 12.0 eV, 11, and 4.5 eV, respectively. The  $f(E_{\text{ph}}, h\gamma)$  values (in arbitrary units) of Cu are calculated with corresponding parameters ( $E_{\text{ph}}$ ,  $h\gamma$ ,  $g(E_{\text{ph}}h\gamma)$  [25],  $E_{\text{F}}$ ,  $\Phi$ ) and Eqs. (6) and (21). Comparisons between these calculated  $f(E_{\text{ph}}, h\gamma)$  of Cu and corresponding experimental ones [25] are shown in Fig. 5.

In the case that  $N_0$  photons at  $\gamma < (E_{\text{F}} + E_{\text{g}})/h$  enter into metals, the electrons with  $E$  in the range of  $[(E_{\text{F}} + \Phi)h, (E_{\text{F}} + \Phi)]$  absorbing one  $h\gamma$  photon have  $E_{\text{ph}}$  in the range of  $[(E_{\text{F}} + \Phi), (E_{\text{F}} + \Phi + h\gamma)]$ , and the photo-emitted electrons with  $E_{\text{ph}}$  in the range of  $[(E_{\text{F}} + \Phi), (E_{\text{F}} + \Phi + h\gamma)]$  may escape into vacuum. Thus, from Eq. (21), it is known that in the case that  $N_0$  photons at  $\gamma < (E_{\text{F}} + E_{\text{g}})/h$  enter perpendicularly into metals, the number of photo-emitted electrons can be written as



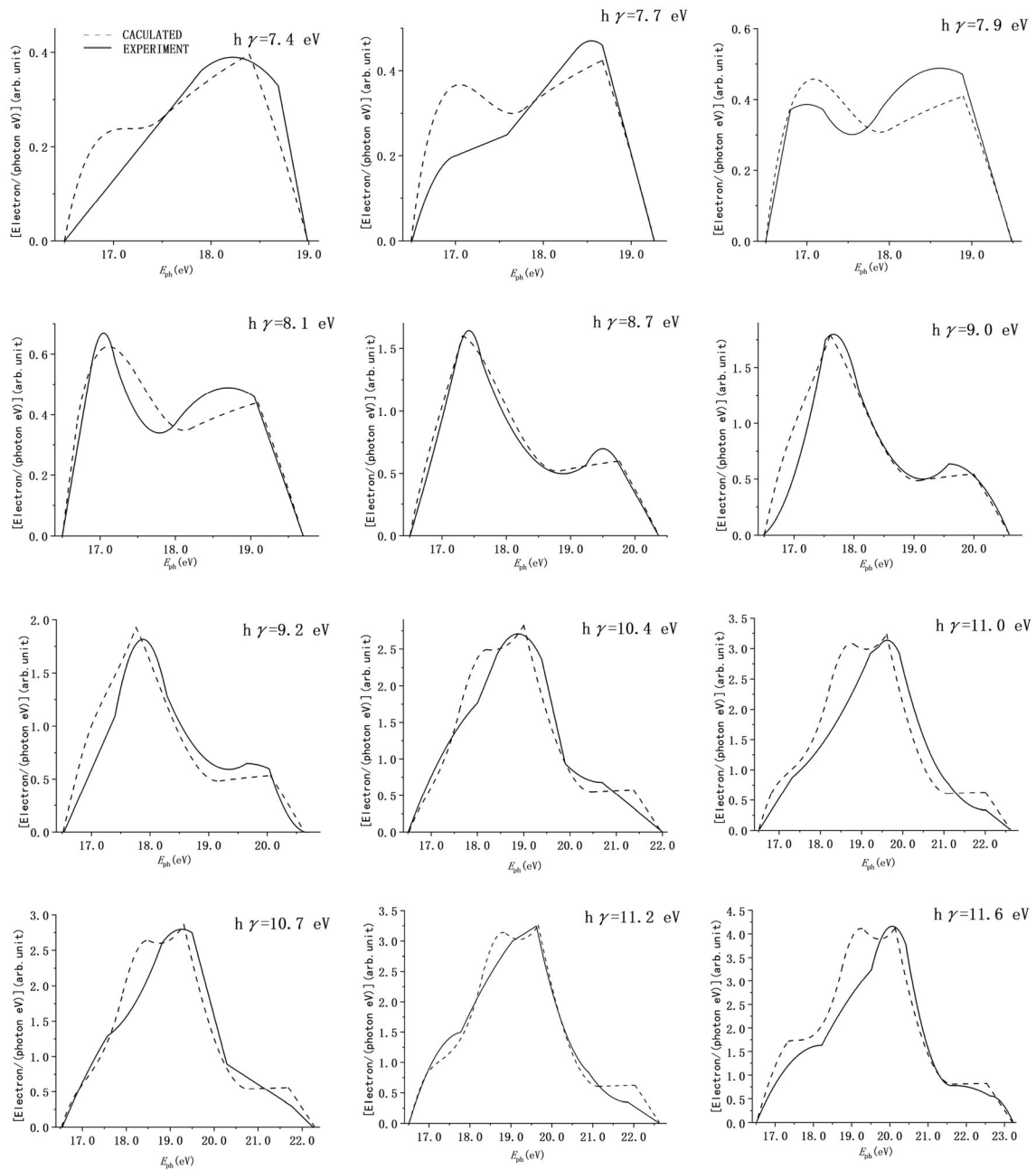


**Fig. 4** Comparisons between the  $f(E_{ph}, h\gamma)$  values of Au calculated using Eq. (21) and experimental ones

$$N_{\text{electrons}1} = \frac{C_\gamma \rho N_A}{A_x} \int_{(EF+\Phi)}^{(EF+\Phi+h\gamma)} \left\{ N_0 g(E_{ph} - h\gamma) \lambda(E_{ph}, h\gamma) (1 - e^{-5}) \left[ 1 - \left( \frac{E_F + \Phi}{E_{ph}} \right)^{0.5} \right] \right\} dE_{ph}. \tag{22}$$

Equations (21)–(22) are deduced on the basis of the assumption that the number of photons at any  $x$  equals  $N_0$ , but in fact, the number of photons at  $x$  decreases with

increasing  $x$ . Thus, from the characteristics of electron emission and the prerequisite of deducing Eq. (22), it is known that in the case that  $N_0$  photons at  $\gamma < (E_F + E_g)/h$  enter perpendicularly into metals, the real number of photo-emitted electrons is less than the value of Eq. (22) and should be written as

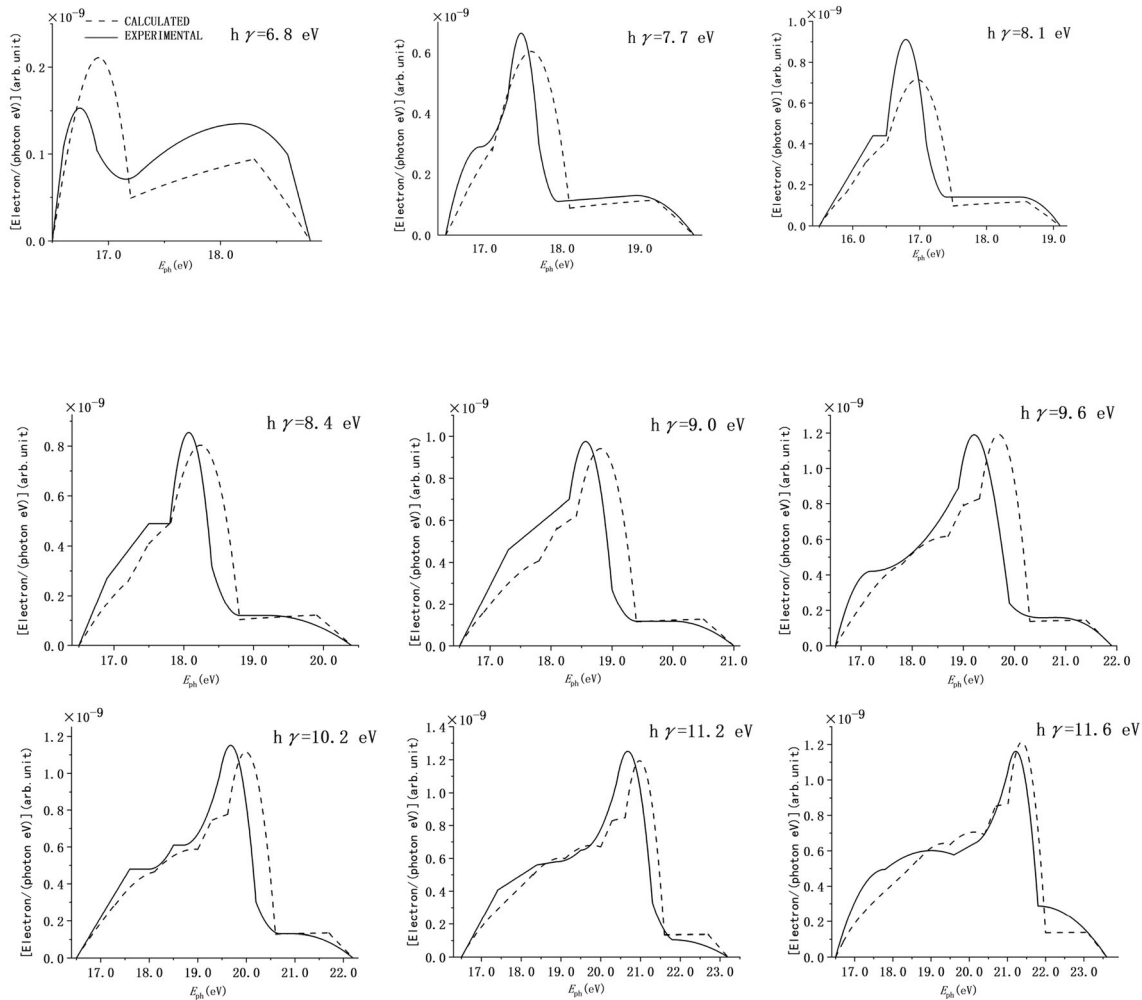


**Fig. 5** Comparisons between the  $f(E_{ph}, h\gamma)$  values of Cu calculated using Eq. (21) and experimental ones

$$N_{\text{electrons}2} = \frac{K(\gamma)C_{\gamma}\rho N_A}{A_x} \int_{(EF+\Phi)}^{(EF+\Phi+h\gamma)} \left\{ N_0 g(E_{ph} - h\gamma) \lambda(E_{ph}, h\gamma) \right. \\ \left. (1 - e^{-5}) \left[ 1 - \left( \frac{E_F + \Phi}{E_{ph}} \right)^{0.5} \right] \right\} dE_{ph}. \tag{23}$$

For a given  $\gamma$  and metal,  $K(\gamma)$  is a constant that is less than 1.0.

According to Eq. (23) and the three-step processes of photo-emission, it is known that in the case that  $N_0$  photons at  $\gamma < (E_F + E_g)/h$  enter perpendicularly into metals, the number of internal photo-excited electrons reaching the emission surface can be written as

$$N_{\text{reach}2} = \frac{K(\gamma)C_{\gamma}\rho N_A}{A_x} \int_{(EF+\Phi)}^{(EF+\Phi+h\gamma)} [N_0 g(E_{ph} - h\gamma) \lambda(E_{ph}, h\gamma) (1 - e^{-5})] dE_{ph}. \tag{24}$$

Based on Eqs. (6) and (23), it is known that in the case that  $N_0$  photons at  $\gamma < (E_F + E_g)/h$  enter perpendicularly into metals, the total escape depth of photo-emitted electrons can be written as

$$N_{\text{depth}2} = \frac{K(\gamma)C_{\gamma}\rho N_A}{A_x} \int_{(EF+\Phi)}^{(EF+\Phi+h\gamma)} \left\{ N_0 g(E_{ph} - h\gamma) \right. \\ \left. (\lambda(E_{ph}, h\gamma))^2 (1 - e^{-5}) \left[ 1 - \left( \frac{E_F + \Phi}{E_{ph}} \right)^{0.5} \right] \right\} dE_{ph}. \tag{25}$$

According to the fact that the photo-emitted electrons with  $E$  have  $E_{vac} = (E_{ph} - E_F - \Phi)$  and Eq. (23), it is known that in the case that  $N_0$  photons at  $\gamma < (E_F + E_g)/h$  enter perpendicularly into metals, the total  $E_{vac}$  of photo-emitted electrons can be written as

$$N_{\text{energy}2} = \frac{K(\gamma)C_\gamma\rho N_A}{A_z} \int_{(E_F+\Phi)}^{(E_F+\Phi+h\gamma)} \{N_0g(E_{\text{ph}} - h\gamma) (E_{\text{ph}} - E_F - \Phi)\lambda(E_{\text{ph}}, h\gamma)(1 - e^{-5}) \left[1 - \left(\frac{E_F + \Phi}{E_{\text{ph}}}\right)^{0.5}\right]\} dE_{\text{ph}} \tag{26}$$

Based on the definition of  $B$  and Eqs. (23) and (24),  $B$  can be expressed as

$$B = N_{\text{electrons}2}/N_{\text{reach}2}. \tag{27}$$

Based on the definition of  $\lambda$  and Eqs. (23) and (25),  $\lambda$  can be written as

$$\lambda = N_{\text{depth}2}/N_{\text{electrons}2}. \tag{28}$$

Based on the definition of  $\lambda$  and Eqs. (23) and (26),  $E_{\text{mean}}$  can be expressed as

$$E_{\text{mean}} = N_{\text{energy}2}/N_{\text{electrons}2}. \tag{29}$$

The  $B$  values of Au calculated with parameters of Au ( $h\gamma$ ,  $g(E_{\text{ph}}h\gamma)$ ,  $E_F$  and  $\Phi$ ) and Eqs. (6), (23), (24), and (27) are shown in Table 3. The  $\lambda$  values of Au calculated with parameters of Au ( $h\gamma$ ,  $g(E_{\text{ph}}h\gamma)$ ,  $E_F$  and  $\Phi$ ) and Eqs. (6), (23), (25) and (28) are shown in Table 3. The  $E_{\text{mean}}$  values of Au calculated with parameters of Au ( $h\gamma$ ,  $g(E_{\text{ph}}h\gamma)$ ,  $E_F$  and  $\Phi$ ) and Eqs. (6), (23), (26) and (29) are shown in Table 3. Using the same method, the  $B$ ,  $\lambda$ , and  $E_{\text{mean}}$  values of Ni and Cu are calculated and shown in Tables 4 and 5, respectively.

As is done for the first SEE model, the lower limit of the integral in Eqs. (23)–(26) should be replaced with “ $h\gamma$ ” when calculating the corresponding parameters ( $B$ ,  $\lambda$  and  $E_{\text{mean}}$ ) at  $h\gamma > 11.0$  eV for Ni.

**Table 3** The parameters of Au calculated using the second SEE model

$h\gamma$ (eV)	$C_\gamma$ ( $10^{-23}$ m <sup>2</sup> )	$\lambda_\gamma$ ( $10^{-9}$ m)	$\lambda$ ( $10^{-9}$ m)	$B$	$E_{\text{mean}}$ (eV)
7.4	45	4.24	2.61	0.0231	1.35
7.7	45.5	4.01	2.58	0.0224	1.42
7.9	48	3.70	2.58	0.0219	1.45
8.1	48.4	3.59	2.58	0.0223	1.46
8.7	49.1	3.34	2.53	0.0262	1.58
9.0	51.2	3.15	2.48	0.0285	1.67
9.2	55.1	2.89	2.45	0.0303	1.74
10.4	53.0	2.92	2.19	0.0459	2.35
10.7	59.4	2.61	2.13	0.0485	2.52
11.0	64.9	2.38	2.07	0.0503	2.69
11.2	66.3	2.33	2.04	0.0515	2.79
11.5	67.6	2.28	2.0	0.0533	2.95

**Table 4** The parameters of Ni calculated using the second SEE model

$h\gamma$ (eV)	$C_\gamma$ ( $10^{-23}$ m <sup>2</sup> )	$\lambda_\gamma$ ( $10^{-9}$ m)	$\lambda$ ( $10^{-9}$ m)	$B$	$E_{\text{mean}}$ (eV)
7.6	12.2	9.01	1.74	0.0512	1.81
8.0	18.3	2.99	1.68	0.0569	2.03
8.6	22.2	4.95	1.59	0.0648	2.35
9.2	27.8	3.94	1.52	0.0683	2.65
9.8	30.8	3.56	1.48	0.0676	2.88
10.4	45.1	2.43	1.46	0.0720	3.06
11.0	46.1	2.38	1.4	0.0847	3.31
11.6	36.2	3.03	1.32	0.106	3.69

According to the simple theories of transport and escape of internal secondary electrons, the probability that an internal secondary electron, which is excited at  $x$ , can reach the emission surface and pass over the surface barrier of a metal into vacuum can be written as [41–44]

$$f(x)_s = B_s e^{-x/\lambda_s}, \tag{30}$$

where  $B_s$  is the mean probability that an internal secondary electron escapes into vacuum upon reaching the emission surface, and  $\lambda_s$  is the mean escape depth of secondary electrons.

Based on Eq. (30) and the fact that SEEs and photo-emission have common mechanisms of transport and escape [6, 7], similarly, the probability that an internal photo-emitted electron, which is excited at  $x$ , can reach the emission surface and pass over the surface barrier of metal can be written as

$$f(x)_{\text{ph}} = B e^{-x/\lambda}. \tag{31}$$

Thus, according to the three-step processes of photo-emission and Eqs. (4) and (31), it is known that in the case that  $N_0$  photons at  $\gamma < (E_F + E_g)/h$  enter perpendicularly into metals, the number of photo-emitted electrons can be written as

$$N_{\text{electrons}} = \int_0^\infty (n(x)f(x)_{\text{ph}}) dx = N_0 \alpha_{\text{ph}\gamma} B \int_0^\infty [e^{-(\alpha_\gamma + \frac{1}{\lambda})x}] dx = \frac{N_0 B \lambda \alpha_{\text{ph}\gamma}}{1 + \lambda \alpha_\gamma}. \tag{32}$$

Therefore, from Eq. (32) and the definition of  $AQE(h\gamma)$ , the  $AQE(h\gamma)$  can be written as

$$AQE(h\gamma) = \frac{B \lambda \alpha_{\text{ph}\gamma}}{1 + \lambda \alpha_\gamma}. \tag{33}$$

**Table 5** The parameters of Cu calculated using the second SEE model

$h\gamma$ (eV)	Experimental $AQE(h\gamma)$ [25]	$n\%$ [25]	$m\%$ [25]	$C_\gamma$ ( $10^{-23}$ m <sup>2</sup> )	$\lambda_\gamma$ ( $10^{-9}$ m)	$\lambda$ ( $10^{-9}$ m)	$B$	$E_{\text{mean}}$ (eV)
6.8	$1.6 \times 10^{-3}$	0.694	0.128	43.1	3.58	2.92	0.0193	1.32
7.4	$2.6 \times 10^{-3}$	0.763	0.237	28.9	4.86	2.92	0.0223	1.35
7.7	$3.0 \times 10^{-3}$	0.788	0.277	22.8	5.95	2.86	0.0263	1.45
8.1	$3.9 \times 10^{-3}$	0.817	0.324	21.5	6.09	2.74	0.0317	1.65
8.4	$4.5 \times 10^{-3}$	0.836	0.361	20.4	6.28	2.65	0.0351	1.81
9.0	$5.8 \times 10^{-3}$	0.873	0.434	19.1	6.43	2.49	0.0418	2.15
9.6	$6.8 \times 10^{-3}$	0.906	0.506	17.2	6.87	2.34	0.0479	2.49
10.2	$7.8 \times 10^{-3}$	0.936	0.570	15.9	7.21	2.21	0.0546	2.84
11.2	$8.8 \times 10^{-3}$	0.976	0.681	13.5	8.13	2.02	0.0634	3.43
11.6	$9.2 \times 10^{-3}$	0.989	0.731	12.8	8.43	1.96	0.066	3.65

Based on the energy band structures of metal shown in Fig. 1, the calculated  $g(E)$ , the values of  $E_F$  and  $\Phi$ , the law of energy conservation, and the fact that  $\gamma$  is  $< (E_F + E_g)/h$ , we can calculate the relative number of electrons in the conduction band of a metal which may absorb one photon and become internal photo-emitted electrons. For example, when the photons at  $h\gamma = 7.4$  eV enter into Au with  $E_F = 11.6$  eV and  $\Phi = 4.9$  eV, it is known that the electrons absorbing one photon and having  $E \geq [E_F - (7.4 \text{ eV} - \Phi)]$  (i.e., 9.1 eV) may have enough energy to become internal photo-emitted electrons. Thus, based on the  $g(E)$  value of Au, the fact that the electrons with  $E$  9.1 eV may become internal photo-emitted electrons and the fact that the  $E_F$  and  $\Phi$  values of Au equal 11.6 eV and 4.9 eV, respectively, we can calculate the  $m\%$  electrons in the conduction band of Au which may absorb one photon and become internal photo-emitted electrons by calculating, and the calculated  $m\%$  at  $h\gamma = 7.4$  eV of Au equals 0.0734. Using the same method, the  $m\%$  at different  $h\gamma$  values of Au, Ni, and Cu can be calculated and are shown in Tables 1, 2, and 5, respectively. Therefore, from the definition of  $\alpha_{\text{ph}\gamma}$  and the fact that the probability that the electron in the conduction band of a given metal absorbs one photon at a given  $\gamma$  can be considered as a constant  $C_\gamma$ , in the case that photons at  $\gamma < (E_F + E_g)/h$  enter perpendicularly into metals, the  $\alpha_{\text{ph}\gamma}$  value of Eq. (33) can be expressed as

$$\alpha_{\text{ph}\gamma} = (s\rho N_A C_\gamma m\%) / A_\alpha. \quad (34)$$

Note that in the case that photons at  $\gamma < (E_F + E_g)/h$  enter perpendicularly into metals, the  $\alpha_\gamma$  value of Eq. (33) is expressed as Eq. (2).

$\alpha_\gamma$  of NEAS equals  $\alpha_{\text{ph}\gamma}$  [22–24]. Thus, from Eq. (33),  $AQE(h\gamma)$  from NEAS can be written as

$$AQE(h\gamma) = \frac{B\lambda\alpha_\gamma}{1 + \lambda\alpha_\gamma}. \quad (35)$$

It is well known that excited electrons (including electron-induced electrons, ion-induced electrons, and photo-

excited electrons) with different  $E$  values have different values of mean escape depth and mean escape probability [6, 7, 13, 26, 32–37, 45]. Thus, from the physical mechanisms of transport and escape of excited electrons, it is known that the process that Eqs. (30)–(31) use to express  $f(x)$  in the courses of deducing some formulas [41–44] is an approximate process; where  $f(x)$  is the probability that an electron excited at  $x$  escapes into a vacuum. In other words, there is the approximation that Eq. (31) is used to express  $f(x)_{\text{ph}}$  made in the courses of deducing Eq. (33). Equation (6) is derived from Eq. (5), which is correct [34, 35] in the case that  $E_{\text{am}}$  is much larger than 1.0 eV, and Eq. (8) and Eq. (31) are derived from Eq. (7) [36, 37] and Eq. (30) [41–44], which are also correct. Thus, Eqs. (6), (8), and (31) are correct. Therefore, from the fact there is an approximation made while deducing Eq. (33) and Eqs. (13) and (33), it can be concluded that Eq. (13) in the case that  $E_{\text{mean}}$  is much larger than 1.0 eV and (32) is theoretically correct, and that Eq. (13) in the case that  $E_{\text{mean}}$  is much larger than 1.0 eV is more accurate than Eq. (33).

Some authors assumed that the negative electron affinity photo-emission process can be described by a diffusion model in which  $AQE(h\gamma)$  from NEAS can be expressed as Eq. (35) [22–24], and they successfully used Eq. (35) to analyze the parameters of the negative electron affinity photo-emission [22–24]. That is, Eq. (35) is experimentally proven. Thus, from deducing Eqs. (33) and Eq. (35), the conclusion that Eq. (33) is theoretically correct and the relation between Eq. (33) and Eq. (35), it can be concluded that Eq. (33) is further proven to be correct.

## 5 Results and discussion

It can be seen from Fig. 2 that the calculated  $f(E_{\text{ph}}, h\gamma)$  values of Au agree well with the experimental ones [20] at  $h\gamma = 8.1$ – $11.6$  eV, but not at  $h\gamma = 7.4$ – $7.9$  eV. It can also be seen from Fig. 3 and the calculated  $f(E_{\text{ph}}, h\gamma)$  value of

Ni in Fig. 13 of Ref. [21] that both calculations of Ni are in good agreement at  $h\gamma = 9.2\text{--}11.6$  eV, but not at  $h\gamma = 7.6\text{--}8.6$  eV. Thus, it can be concluded that Eq. (10) can be used to express the  $f(E_{\text{ph}}, h\gamma)$  from Au at  $h\gamma = 8.1\text{--}11.6$  eV and Ni at  $h\gamma = 9.2\text{--}11.6$  eV, and that Eq. (10) can at least express the relative number of photo-emitted electrons with  $E_{\text{ph}}$  in the cases that  $N_0$  photons at  $h\gamma = 8.1\text{--}11.6$  eV enter into Au and that  $N_0$  photons at  $h\gamma = 9.2\text{--}11.6$  eV enter into Ni. Therefore, according to the relation between Eq. (10) and Eqs. (12)–(16), it is concluded that Eqs. (12)–(16) can at least be used to express the relative values of  $N_{\text{electrons}}$ ,  $AQE(h\gamma)$ ,  $N_{\text{reach}}$ ,  $N_{\text{depth}}$ , and  $N_{\text{energy}}$  from Au at  $h\gamma = 8.1\text{--}11.6$  eV and Ni at  $h\gamma = 9.2\text{--}11.6$  eV. Then, from Eqs. (17)–(19), it can be concluded that Eqs. (17)–(19) can be used to calculate the  $B$ ,  $\lambda$ , and  $E_{\text{mean}}$  values of Au at  $h\gamma = 8.1\text{--}11.6$  eV and Ni at  $h\gamma = 9.2\text{--}11.6$  eV, respectively. That is, the  $B$ ,  $\lambda$ , and  $E_{\text{mean}}$  values of Au at  $h\gamma = 8.1\text{--}11.5$  eV and Ni at  $h\gamma = 9.2\text{--}11.6$  eV calculated with Eqs. (17)–(19) and shown in Tables 1 and 2 are correct.

The  $AQE(h\gamma)$  values from Au and Ni are calculated using Eqs. (2), (33), and (34) as well as corresponding parameters ( $s$ ,  $N_{\text{A}}$ ,  $\rho$ ,  $A_{\text{x}}$ ,  $B$ ,  $\lambda$ ,  $C_{\gamma}$  calculated using Eq. (13),  $m\%$ , and  $n\%$  shown in Tables 1 and 2). Further, the calculated  $AQE(h\gamma)$  values from Au and Ni are shown in Tables 1 and 2. From Tables 1 and 2, it is known that the calculated  $AQE(h\gamma)$  from Au at  $h\gamma = 7.4\text{--}11.5$  eV and Ni at  $h\gamma = 7.6\text{--}11.6$  eV are in agreement with the corresponding experimental ones [20, 21]. Thus, from the conclusions that the  $B$  and  $\lambda$  of Au at  $h\gamma = 8.1\text{--}11.5$  eV and Ni at  $h\gamma = 9.2\text{--}11.6$  eV calculated with Eqs. (17)–(18) are correct, and the conclusion that Eq. (33) is correct, it can be concluded that the  $C_{\gamma}$  values of Au at  $h\gamma = 8.1\text{--}11.5$  eV and Ni at  $h\gamma = 9.2\text{--}11.6$  eV calculated with Eq. (13) are correct. Therefore, from the conclusions that Eq. (13) can at least be used to express the relative values of  $AQE(h\gamma)$  from Au at  $h\gamma = 8.1\text{--}11.5$  eV and Ni at  $h\gamma = 9.2\text{--}11.6$  eV, it can be concluded that Eq. (13) can also be used to express the absolute values of  $AQE(h\gamma)$  from Au at  $h\gamma = 8.1\text{--}11.5$  eV and Ni at  $h\gamma = 9.2\text{--}11.6$  eV. From the conclusions that the  $C_{\gamma}$  values of Au at  $h\gamma = 8.1\text{--}11.5$  eV and Ni at  $h\gamma = 9.2\text{--}11.6$  eV calculated with Eq. (13) are correct, and the fact that the  $\lambda_{\gamma}$  values of Au and Ni are calculated with Eq. (2) and corresponding  $C_{\gamma}$  calculated with Eq. (13), it can be concluded that the  $\lambda_{\gamma}$  values of Au at  $h\gamma = 8.1\text{--}11.5$  eV and Ni at  $h\gamma = 9.2\text{--}11.6$  eV calculated with Eq. (2) are also correct.

From the conclusion that the  $C_{\gamma}$  values of Ni at  $h\gamma = 9.2\text{--}11.6$  eV calculated with Eq. (13) are correct and the fact that the  $\lambda_{\gamma}$  values of Ni are calculated with Eq. (2) and the  $C_{\gamma}$  values of Ni calculated with Eq. (13), it can be concluded that the  $\lambda_{\gamma}$  of Ni at  $h\gamma = 9.2\text{--}11.6$  eV calculated with Eq. (2) is also correct. From the comparison between the calculated  $AQE(h\gamma)$  from Au at  $h\gamma = 8.1\text{--}11.5$  eV and

$AQE(h\gamma)$  from Ni at  $h\gamma = 9.2\text{--}11.6$  eV shown in Tables 1, 2 and experimental ones [20, 21] shown in Tables 1, 2, it is known that the relative differences between the calculated  $AQE(h\gamma)$  and experimental ones [20, 21] are within the range of 5–15%. From the conclusion that Eq. (13) is more accurate than Eq. (33), it can be assumed that the differences between experimental  $AQE(h\gamma)$  and ones calculated with Eq. (33) and  $C_{\gamma}$  calculated with Eq. (13) mainly result from the approximation of Eq. (33). Therefore, the errors in the  $C_{\gamma}$  values of metals calculated with Eq. (13) can be estimated to be 5%.

It can be seen from Fig. 4 that the calculated  $f(E_{\text{ph}}, h\gamma)$  values of Au agree well with experimental ones [20] at  $h\gamma = 8.1\text{--}11.6$  eV, but not at  $h\gamma = 7.4\text{--}7.9$  eV. It can also be seen from Fig. 3 and the calculated  $f(E_{\text{ph}}, h\gamma)$  of Ni in Fig. 13 of Ref. [21], it is known that both the  $f(E_{\text{ph}}, h\gamma)$  of Ni calculated in Ref. 21 and the  $f(E_{\text{ph}}, h\gamma)$  of Ni calculated with Eq. (21) are in good agreement at  $h\gamma = 9.2\text{--}11.6$  eV but not at  $h\gamma = 7.6\text{--}8.6$  eV. Thus, it can be concluded that Eq. (21) can be used to express the  $f(E_{\text{ph}}, h\gamma)$  from Au at  $h\gamma = 8.1\text{--}11.6$  eV and Ni at  $h\gamma = 9.2\text{--}11.6$  eV, and that Eq. (21) can be used to express the relative number of photo-emitted electrons with  $E_{\text{ph}}$  in the cases that photons at  $h\gamma = 8.1\text{--}11.6$  eV enter into Au and that photons at  $h\gamma = 9.2\text{--}11.6$  eV enter into Ni. Therefore, from the relation between Eq. (21) and Eqs. (23)–(26), it can be concluded that Eqs. (23)–(26) can be used to express the relative values of  $N_{\text{electrons}2}$ ,  $N_{\text{reach}2}$ ,  $N_{\text{depth}2}$ , and  $N_{\text{energy}2}$  from Au at  $h\gamma = 8.1\text{--}11.6$  eV and Ni at  $h\gamma = 9.2\text{--}11.6$  eV. Then, from deducing Eqs. (27)–(29), it is determined that Eqs. (27)–(29) can be used to calculate the  $B$ ,  $\lambda$ , and  $E_{\text{mean}}$  values of Au at  $h\gamma = 8.1\text{--}11.6$  eV and Ni at  $h\gamma = 9.2\text{--}11.6$  eV. That is, the  $B$ ,  $\lambda$  and  $E_{\text{mean}}$  values of Au at  $h\gamma = 8.1\text{--}11.5$  eV and Ni at  $h\gamma = 9.2\text{--}11.6$  eV calculated from Eqs. (27)–(29) and shown in Tables 3 and 4 are correct.

The  $C_{\gamma}$  values of Au calculated with Eqs. (2), (33), and (34),  $s = 11$ ,  $N_{\text{A}}$ ,  $\rho$ ,  $A_{\text{x}}$ , parameters ( $m\%$ ,  $n\%$ , experimental  $AQE(h\gamma)$  [20] shown in Table 1 and parameters ( $B$ ,  $\lambda$ ) shown in Table 3 are shown in Table 3; the  $\lambda_{\gamma}$  values of Au calculated with Eq. (2),  $s = 11$ ,  $N_{\text{A}}$ ,  $\rho$ ,  $A_{\text{x}}$ ,  $C_{\gamma}$  shown in Table 3 and  $n\%$  shown in Table 1 are shown in Table 3. The  $C_{\gamma}$  values of Ni calculated with Eqs. (2), (33), and (34),  $s = 10$ ,  $N_{\text{A}}$ ,  $\rho$ ,  $A_{\text{x}}$ , parameters ( $m\%$ ,  $n\%$ , experimental  $AQE(h\gamma)$  [21]) shown in Table 2 and parameters ( $B$ ,  $\lambda$ ) shown in Table 4 are shown in Table 4; the  $\lambda_{\gamma}$  values of Ni calculated with Eq. (2),  $s = 10$ ,  $N_{\text{A}}$ ,  $\rho$ ,  $A_{\text{x}}$ ,  $C_{\gamma}$  shown in Table 4 and  $n\%$  shown in Table 2 are shown in Table 4. According to the conclusion that the  $B$  and  $\lambda$  values of Au at  $h\gamma = 8.1\text{--}11.5$  eV shown in Table 3 and the  $B$  and  $\lambda$  of Ni at  $h\gamma = 9.2\text{--}11.6$  eV shown in Table 4 are correct and the fact that Eq. (33) is correct, it is determined that the  $C_{\gamma}$  values at  $h\gamma = 8.1\text{--}11.5$  eV for Au shown in Table 3 and

the  $C_\gamma$  at  $h\gamma = 9.2\text{--}11.6$  eV of Ni shown in Table 4, which are calculated with Eq. (33), are reasonable. From the estimation that errors in the  $C_\gamma$  values of Au shown in Table 1 are about 5% and the comparison between  $C_\gamma$  at  $h\gamma = 8.1\text{--}11.5$  eV for Au shown in Table 3 and those in Table 1, it can be estimated that the errors in  $C_\gamma$  at  $h\gamma = 8.1\text{--}11.5$  eV for Au calculated using Eq. (33) and shown in Table 3 are about 20%. Based on the estimation that the errors in  $C_\gamma$  for Ni shown in Table 2 are about 5%, and the comparison between  $C_\gamma$  at  $h\gamma = 9.2\text{--}11.6$  eV for Ni shown in Table 4 and those shown in Table 2, it can be estimated that the errors in  $C_\gamma$  at  $h\gamma = 9.2\text{--}11.6$  eV for Ni calculated using Eq. (33) and shown in Table 4 are about 30%.

It can be seen from Fig. 5 that the calculated  $f(E_{\text{ph}}, h\gamma)$  values of Cu are in good agreement with experimental ones [25] at  $h\gamma = 7.7\text{--}11.6$  eV, but not at  $h\gamma = 6.8$  eV. Thus, it is concluded that Eq. (21) can be used to express the  $f(E_{\text{ph}}, h\gamma)$  values from Cu at  $h\gamma = 7.7\text{--}11.6$  eV. Therefore, from the relation between Eq. (21) and Eqs. (23)–(26), it can be concluded that Eqs. (23)–(26) can at least be used to express the relative values of  $N_{\text{electrons}2}$ ,  $N_{\text{reach}2}$ ,  $N_{\text{depth}2}$ , and  $N_{\text{energy}2}$  from Cu at  $h\gamma = 7.7\text{--}11.6$  eV. Then, from determining Eqs. (27)–(29), it can be concluded that Eqs. (27)–(29) can be used to calculate the  $B$ ,  $\lambda$ , and  $E_{\text{mean}}$  values of Cu at  $h\gamma = 7.7\text{--}11.6$  eV. That is, the  $B$ ,  $\lambda$ , and  $E_{\text{mean}}$  values of Cu at  $h\gamma = 7.7\text{--}11.6$  eV calculated using Eqs. (27)–(29) and shown in Table 5 are correct.

The  $C_\gamma$  values of Cu calculated with Eqs. (2), (33), and (34),  $s = 11$ ,  $N_A$ ,  $\rho$ ,  $A_\alpha$ , parameters ( $m\%$ ,  $n\%$ , experimental  $AQE(h\gamma)$  [25],  $B$ ,  $\lambda$ ) are shown in Table 5. The  $\lambda_\gamma$  value of Cu calculated with Eq. (2),  $s = 11$ ,  $N_A$ ,  $\rho$ ,  $A_\alpha$ ,  $C_\gamma$  shown in Table 5 and  $n\%$  shown in Table 5 are also shown in Table 5. From the conclusion that the  $B$  and  $\lambda$  values of Cu at  $h\gamma = 7.7\text{--}11.6$  eV shown in Table 5 are correct and the fact that Eq. (33) is correct, it can be concluded that the  $C_\gamma$  values at  $h\gamma = 7.7\text{--}11.6$  eV of Cu calculated using Eq. (33) and shown in Table 5 are reasonable. There is no  $C_\gamma$  at  $h\gamma = 7.7\text{--}11.6$  eV for Cu calculated by other authors or using other current methods. Thus, we cannot estimate the errors in  $C_\gamma$  at  $h\gamma = 7.7\text{--}11.6$  eV for Cu calculated using Eq. (33). The relative differences among the  $C_\gamma$  values at  $h\gamma < 50$  eV obtained by different authors can reach about 200% or more [19]. Thus, from the estimations that the errors in  $C_\gamma$  at  $h\gamma = 8.1\text{--}11.5$  eV for Au shown in Table 3 are about 20%, and that the errors in  $C_\gamma$  at  $h\gamma = 9.2\text{--}11.6$  eV for Ni shown in Table 4 are about 30%, it can be concluded that the method of calculating  $C_\gamma$  for metals using Eq. (33) is more accurate. According to the estimation that the errors in  $C_\gamma$  for metals calculated using Eq. (13) are about 5%, it can be concluded that the method of calculating  $C_\gamma$  for metals using Eq. (13) is very accurate. From the perspective of accuracy of the calculated  $C_\gamma$ , it appears that the method of calculating  $C_\gamma$  with Eq. (13)

presented in the first SEE model is better than that of calculating  $C_\gamma$  with Eq. (33) presented in the second SEE model. However, it is important to note that in the case that the absolute  $g(E_{\text{ph}}h\gamma)$  is not known, the method of calculating the  $C_\gamma$  value for metals using Eq. (13) cannot be used to calculate  $C_\gamma$ , but the method of calculating the  $C_\gamma$  value for metals using Eq. (33) can be used to calculate  $C_\gamma$ . For example, because only the relative  $g(E_{\text{ph}}h\gamma)$  value of Cu is known in this study [25], the  $C_\gamma$  value at  $h\gamma = 7.7\text{--}11.6$  eV for Cu can only be calculated using the method of calculating the  $C_\gamma$  value for metals with Eq. (33). It is also important to note that in the cases that  $AQE(h\gamma)$  are not known, the first SEE model cannot be used to calculate  $f(E_{\text{ph}}, h\gamma)$ ,  $B$ ,  $\lambda$ , and  $E_{\text{mean}}$ , but the second SEE model can be used to do so.

From the comparison between Fig. 2 and Fig. 4 and the comparison between the  $f(E_{\text{ph}}, h\gamma)$  values of Ni calculated with Eq. (10) and those calculated with Eq. (21) in Fig. 3, it is known that the differences between  $f(E_{\text{ph}}, h\gamma)$  values for Au and Ni calculated with Eq. (10) and those calculated with Eq. (21) are very small. From Tables 1, 2, 3, 4, it is seen that the  $B$ ,  $\lambda$ , and  $E_{\text{mean}}$  values of Au and Ni calculated with Eqs. (17)–(19) are approximately equal to those calculated with Eqs. (27)–(29). That is, Eqs. (9) and (17)–(19) deduced in the first SEE model can be replaced with Eqs. (20) and (27)–(29) deduced in the second SEE model, respectively, and vice versa. From the above comparison among  $f(E_{\text{ph}}, h\gamma)$ ,  $B$ ,  $\lambda$ , and  $E_{\text{mean}}$  for Au and Ni, and the courses of calculating  $f(E_{\text{ph}}, h\gamma)$ ,  $B$ ,  $\lambda$ , and  $E_{\text{mean}}$  for Au, Cu, and Ni, we found that the values of  $C_\gamma$  have little influence on the shape of  $f(E_{\text{ph}}, h\gamma)$  and the values of  $B$ ,  $\lambda$ , and  $E_{\text{mean}}$ , but that both  $g(E_{\text{ph}}h\gamma)$  and  $h\gamma$  significantly influence them. For example, the shape of  $g(E_{\text{ph}}h\gamma)$  significantly influences the shape of  $f(E_{\text{ph}}, h\gamma)$ .

The excited electrons with  $E_{\text{vac}} < 1.0$  eV lose energy mainly by multiple electron–phonon scattering [13, 37, 45, 46]. Electron–phonon scattering loses less energy every time there is scattering, and the excited electrons with  $E_{\text{vac}} < 1.0$  eV may still become emitted electrons after several occurrences of electron–phonon scattering [13, 37, 45, 46]. Thus, if the excited electrons with  $E_{\text{vac}} < 1.0$  eV have more energy, they can travel a greater distance to escape into vacuum. Therefore, the mean escape depth of the excited electrons with  $E_{\text{vac}} < 1.0$  eV is proportional to  $E_{\text{vac}}$  [13, 37, 45, 46]. However, the excited electrons with  $E_{\text{vac}}$  values that are much larger than 1.0 eV lose energy mainly by single electron–electron scattering. Electron–electron scattering results in the loss of a larger amount energy at every scattering, and the excited electrons with  $E_{\text{vac}}$  values much larger than 1.0 eV almost cannot become emitted electrons after single electron–electron scattering [13, 37, 45, 46]. The probability that an excited electron with  $E_{\text{vac}}$  much larger than 1.0 eV

undergoes single electron–electron scattering per unit path length of excited electron is proportional to  $E_{\text{vac}}$  [13, 37, 45, 46]. Thus, the mean escape depth of the excited electrons with  $E_{\text{vac}}$  much larger than 1.0 eV is inversely proportional to  $E_{\text{vac}}$ . Most secondary electrons have energy  $E_{\text{vac}} > 1.0$  eV [32, 33], and  $E_{\text{am}}$  is much larger than 1.0 eV, and the secondary electrons lose energy mainly by single electron–electron scattering. Thus,  $\lambda_s$  is inversely proportional to  $E_{\text{vac}}$ , and the mean escape depth of secondary electrons with  $E_0(0E_0\Phi E_F 1.5E_F)$  can be expressed as Eq. (5). In other words, Eq. (5) is correct in the case that the  $E_{\text{am}}$  is much larger than 1.0 eV. Therefore, from the fact that Eq. (6) is derived from Eq. (5), it can be concluded that Eq. (6) is correct in the case that  $E_{\text{mean}}$  is much larger than 1.0 eV. Then, it is concluded that Eqs. (10), (17)–(19), (21), and (27)–(29) derived from Eq. (6) are also correct in the case that  $E_{\text{mean}}$  is much larger than 1.0 eV. From Tables 1, 2, 3, 4, 5, it can be seen that the  $E_{\text{mean}}$  of Au at  $h\gamma = 8.1$ –11.5 eV, Ni at  $h\gamma = 9.2$ –11.6 eV and Cu at  $h\gamma = 7.7$ –11.6 eV are much larger than 1.0 eV. For this reason,  $f(E_{\text{ph}}, h\gamma)$  calculated here for Au at  $h\gamma = 8.1$ –11.6 eV, Ni at  $h\gamma = 9.2$ –11.6 eV, and Cu at  $h\gamma = 7.7$ –11.6 eV are in good agreement with the corresponding experimental ones and the ones calculated by other authors [20, 21, 25], and the  $B$ ,  $\lambda$ , and  $C_\gamma$  values calculated here for Au at  $h\gamma = 8.1$ –11.5 eV, Ni at  $h\gamma = 9.2$ –11.6 eV and Cu at  $h\gamma = 7.7$ –11.6 eV are correct.

If the metal surfaces are contaminated or if metals have some impurities, the photo-emission from these metals becomes more complex. Thus, it is important to note that we must use experimental  $f(E_{\text{ph}}, h\gamma)$  and  $AQE(h\gamma)$  values of clean and pure metals to investigate the corresponding  $f(E_{\text{ph}}, h\gamma)$ ,  $E_{\text{mean}}$ ,  $B$ ,  $\lambda$  and  $C_\gamma$  in this work, and that the experimental  $f(E_{\text{ph}}, h\gamma)$  and  $AQE(h\gamma)$  used in this work are those of three clean and pure metals [20, 21, 25]. In other words, the two SEE models presented in this work are only suitable for photo-emission from clean and pure metals in the vacuum ultraviolet.

## 6 Conclusion

In this study, Eqs. (10) and (21) for  $f(E_{\text{ph}}, h\gamma)$  from metals have been deduced and proven to be correct for the cases of Au at  $h\gamma = 8.1$ –11.6 eV and Ni at  $h\gamma = 9.2$ –11.6 eV, respectively. Thus, from the relation between Eq. (10) and Eqs. (12)–(16) as well as the relation between Eq. (21) and Eqs. (23)–(26), it is concluded that Eqs. (12)–(16) can at least be used to express the corresponding relative values of  $N_{\text{electrons2}}$ ,  $AQE(h\gamma)$ ,  $N_{\text{reach2}}$ ,  $N_{\text{depth2}}$  and  $N_{\text{energy2}}$ , respectively; and that Eqs. (23)–(26) can be used to express the corresponding relative values of  $N_{\text{electrons2}}$ ,  $N_{\text{reach2}}$ ,  $N_{\text{depth2}}$  and  $N_{\text{energy2}}$ , respectively. Therefore, from determining

Eqs. (17)–(19) and (27)–(29), it can be concluded that Eqs. (17)–(19) and Eqs. (27)–(29) can be used to calculate the  $B$ ,  $\lambda$ , and  $E_{\text{mean}}$  values for Au at  $h\gamma = 8.1$ –11.5 eV and Ni at  $h\gamma = 9.2$ –11.6 eV.

The  $AQE(h\gamma)$  value from Au at  $h\gamma = 7.4$ –11.5 eV and Ni at  $h\gamma = 7.6$ –11.6 eV is calculated using Eqs. (2), (33), and (34), the  $B$  and  $\lambda$  values for Au and Ni calculated with Eqs. (17)–(18), and the  $C_\gamma$  values for Au and Ni calculated using Eq. (13). These calculated  $AQE(h\gamma)$  values from Au and Ni agree well with the corresponding experimental ones. Thus, from the conclusions that the  $B$  and  $\lambda$  values of Au at  $h\gamma = 8.1$ –11.5 eV and Ni at  $h\gamma = 7.6$ –11.6 eV calculated with Eqs. (17)–(18) are correct and the conclusion that Eq. (33) is correct, it can be concluded that the  $C_\gamma$  values of Au at  $h\gamma = 8.1$ –11.5 eV and Ni at  $h\gamma = 7.6$ –11.6 eV calculated with Eq. (13) are correct. Therefore, from the conclusions that Eq. (13) can at least be used to express the relative values of  $AQE(h\gamma)$  from Au at  $h\gamma = 8.1$ –11.5 eV and Ni at  $h\gamma = 7.6$ –11.6 eV, it can be concluded that Eq. (13) can be used to express the absolute values of  $AQE(h\gamma)$  from Au at  $h\gamma = 8.1$ –11.5 eV and Ni at  $h\gamma = 7.6$ –11.6 eV.

The  $C_\gamma$  values of Au are calculated using Eqs. (2), (33), and (34),  $s = 11$ ,  $N_A$ ,  $\rho$ ,  $A_\alpha$ , parameters ( $m\%$ ,  $n\%$ , experimental  $AQE(h\gamma)$ ) shown in Table 1 and parameters ( $B$ ,  $\lambda$ ) shown in Table 3, the  $C_\gamma$  of Ni values are calculated using Eqs. (2), (33), and (34),  $s = 10$ ,  $N_A$ ,  $\rho$ ,  $A_\alpha$ , parameters ( $m\%$ ,  $n\%$ , experimental  $AQE(h\gamma)$ ) shown in Table 2 and parameters ( $B$ ,  $\lambda$ ) shown in Table 4. According to the conclusion that the  $B$  and  $\lambda$  values for Au at  $h\gamma = 8.1$ –11.5 eV shown in Table 3 and the  $B$  and  $\lambda$  values for Ni at  $h\gamma = 9.2$ –11.6 eV shown in Table 4 are correct and the fact that Eq. (33) is correct, it can be concluded that the  $C_\gamma$  values for Au at  $h\gamma = 8.1$ –11.5 eV and Ni at  $h\gamma = 9.2$ –11.6 eV calculated using Eq. (33) are reasonable. From the comparison between the  $C_\gamma$  values for Au at  $h\gamma = 8.1$ –11.5 eV for Au calculated with Eq. (33) and the corresponding ones shown in Table 1, it can be estimated that the errors in the  $C_\gamma$  at  $h\gamma = 8.1$ –11.5 eV for Au calculated with Eq. (33) are about 20%. Based on the comparison between the  $C_\gamma$  values for Ni at  $h\gamma = 9.2$ –11.6 eV for Ni calculated with Eq. (33) and corresponding ones shown in Table 2, it can be estimated that the errors in  $C_\gamma$  at  $h\gamma = 9.2$ –11.6 eV for Ni calculated with Eq. (33) are about 30%.

Equation (21) for the  $f(E_{\text{ph}}, h\gamma)$  at  $h\gamma = 7.7$ –11.6 eV of Cu has been experimentally proven. Thus, from the relation between Eq. (20) and Eqs. (23)–(26), it is concluded that Eqs. (23)–(26) can be used to calculate the relative values of  $N_{\text{electrons2}}$ ,  $N_{\text{reach2}}$ ,  $N_{\text{depth2}}$ , and  $N_{\text{energy2}}$  from Cu at  $h\gamma = 7.7$ –11.6 eV. Therefore, from determining Eqs. (27)–(29), it can be concluded that Eqs. (27)–(29) can be used to calculate  $B$ ,  $\lambda$ , and  $E_{\text{mean}}$  values for Cu at  $h\gamma = 7.7$ –11.6 eV.

The  $C_\gamma$  values for Cu are calculated using Eqs. (2), (33), and (34),  $s = 11$ ,  $N_A$ ,  $\rho$ ,  $A_\alpha$ , parameters ( $m\%$ ,  $n\%$ , experimental  $AQE(h\gamma)$ ) shown in Table 5,  $B$  and  $\lambda$  calculated with Eqs. (27)–(28). From the conclusion that the  $B$  and  $\lambda$  values for Cu at  $h\gamma = 7.7$ – $11.6$  eV calculated with Eqs. (27)–(28) are correct and the fact that Eq. (33) is correct, it can be concluded that the  $C_\gamma$  values at  $h\gamma = 7.7$ – $11.6$  eV for Cu calculated using Eq. (33) are reasonable. The relative differences among the  $C_\gamma$  values at  $h\gamma < 50$  eV obtained by different authors can reach about 200% or more [19]. Thus, from the estimations that the errors in  $C_\gamma$  for Au at  $h\gamma = 8.1$ – $11.5$  eV and Ni at  $h\gamma = 9.2$ – $11.6$  eV calculated using Eq. (33) are about 20% and 30%, it can be concluded that the method of calculating  $C_\gamma$  for metals using Eq. (33) is more accurate. From the estimation that the errors in  $C_\gamma$  for metals calculated using Eq. (13) are about 5%, it can be concluded that the method of calculating  $C_\gamma$  for metals using Eq. (13) is very accurate.

**Author contributions** All authors contributed to the study conception and design. Material preparation, data collection and analysis were performed by Ai-Gen Xie, Yi-Fan Liu and Hong-Jie Dong. The first draft of the manuscript was written by Ai-Gen Xie and all authors commented on previous versions of the manuscript. All authors read and approved the final manuscript.

## References

- X.D. Su, G.L. Zhang, S.P. Xu et al., Attenuation coefficients of gamma and X-rays passing through six materials. *Nucl. Sci. Tech.* **31**, 3 (2020). <https://doi.org/10.1007/s41365-019-0717-9>
- B. Lv, Y. Liu, W. Wu et al., Local large temperature difference and ultra-wideband photothermoelectric response of the silver nanostructure film/carbon nanotube film heterostructure. *Nat. Commun.* **13**, 1835 (2022). <https://doi.org/10.1038/s41467-022-29455-6>
- H.W. Yu, Y.X. Zhang, X.H. Chen et al., Numerical simulation and method study of X-ray litho-density logging. *Nucl. Sci. Tech.* **31**(12), 124 (2020). <https://doi.org/10.1007/s41365-020-00826-2>
- D.Y. Lin, Y.T. Shih, W.C. Tseng et al., Influence of Mn, Fe Co, and Cu doping on the photoelectric properties of 1T HfS<sub>2</sub> crystals. *Materials* **15**, 173 (2022). <https://doi.org/10.3390/ma15010173>
- Y. Lei, B. Du, P. Du et al., The effects of Se/S ratio on the photoelectric properties of nitrogen -doped graphene quantum dots decorated CdS<sub>x</sub>Se<sub>1-x</sub> composites. *Ceram. Int.* **48**, 5280–5288 (2022). <https://doi.org/10.1016/j.ceramint.2021.11.071>
- J. Cazaux, Correlation between the X-ray induced and the electron-induced electron emission yields of insulators. *J. Appl. Phys.* **89**, 8265–8272 (2001). <https://doi.org/10.1063/1.1368867>
- J. Cazaux, Electron and X-ray-induced electron emissions from insulators. *Polym. Int.* **50**, 748–755 (2001). <https://doi.org/10.1002/pi.650>
- Y. Zhang, J. Zhao, H. Wang et al., Single-atom Cu anchored catalysts for photocatalytic renewable H<sub>2</sub> production with a quantum efficiency of 56. *Nat. Commun.* **13**, 58 (2022). <https://doi.org/10.1038/s41467-021-27698-3>
- N.Q. Cai, G.Q. Zhang, C.B. Fu et al., Populating <sup>229m</sup>Th via two-photon electronic bridge mechanism. *Nucl. Sci. Tech.* **32**(6), 59 (2021). <https://doi.org/10.1007/s41365-021-00900-3>
- R. Jiang, X. Wu, H. Liu et al., High-performance orange-red organic light-emitting diodes with external quantum efficiencies reaching 33.5% based on carbonyl-containing delayed fluorescence molecules. *Adv. Sci.* **9**, 2104435 (2022). <https://doi.org/10.1002/advs.202104435>
- H. Mayer, R. Nossek, Die entwicklung der leitfähigkeit und des ausseren lichtelektrischen effektes beim ubergang vom eibzelatom zum kompakten metall. *Z. Physik.* **138**, 353–362 (1954). <https://doi.org/10.1007/BF01340681>
- H. Mayer, R. Nossek, H. Thomas, Le libre parcours moyen des électrons de conductibilité et des électrons photoélectriques mesuré au moyen de la méthode des couches minces. *J. Phys. Radium.* **17**, 204–209 (1956). <https://doi.org/10.1051/jphysrad:01956001703020400>
- Photoemissive Materials: Preparation, Properties, Uses, 1th edition, edited by Sommer A. H., published by John Wiley and Sons, Inc (1968), pages 38–58
- F. Salvat, L. Barjuan, P. Andreo, Inelastic collisions of fast charged particles with atoms: bethe asymptotic formulas and shell corrections. *Phys. Rev. A* **105**(4), 042813 (2022). <https://doi.org/10.1103/PhysRevA.105.042813>
- S. Biswas, B. Förg, L. Ortmann et al., Probing molecular environment through photoemission delays. *Nat. Phys.* **16**(7), 1–6 (2020). <https://doi.org/10.1038/s41567-020-0887-8>
- H.J. Liu, J.C. Wang, D.Y. Cho et al., Giant photoresponse in quantized SrRuO<sub>3</sub> monolayer at oxide interfaces. *ACS Photonics* **5**, 1041–1049 (2018). <https://doi.org/10.1021/acsp Photonics.7b01339>
- D. Sier, G.P. Cousland, R.M. Trevorah et al., High accuracy determination of photoelectric cross sections, X-ray absorption fine structure and nanostructure analysis of zinc selenide using the X-ray extended range technique. *J. Synchrotron. Rad.* **27**, 1262–1277 (2020). <https://doi.org/10.1107/S1600577520010097>
- R. Prasad, Total photon-absorption cross-section measurements at 52.4, 60, 72.2, and 84.4 keV in Al, Fe, Mo, Ag, W, and Pt: Photoelectric cross sections deduced. *Phys. Rev. A.* **18**(5), 2167–2169 (1978). <https://doi.org/10.1103/PhysRevA.18.2167>
- M.C. Han, H.S. Kim, M.G. Pia et al., Validation of cross sections for Monte Carlo simulation of the photoelectric effect. *IEEE. T. Nucl. Sci.* **63**(2), 1117–1146 (2016). <https://doi.org/10.1109/TNS.2016.2521876>
- W.F. Krolkowski, W.E. Spicer, Photoemission studies of the noble metals. II. Gold. *Phys. Rev. B.* **1**(2), 478 (1970). <https://doi.org/10.1103/PhysRevB.1.478>
- A.J. Blodgett Jr., W.E. Spicer, Spicer, Experimental determination of the density of states in nickel. *Phys. Rev.* **146**, 390–402 (1966). <https://doi.org/10.1103/PhysRev.146.390>
- R.U. Martinelli, Secondary emission and photoemission from negative electron affinity GaP: Cs. *J. Appl. Phys.* **45**, 3203–3204 (1974). <https://doi.org/10.1063/1.1663751>
- D.G. Fisher, R.E. Enstrom, J.S. Escher et al., Photoelectron surface escape probability of (Ga, In)As: Cs–O in the 0.9 to [inverted lazy s]1.6  $\mu\text{m}$  range. *J. Appl. Phys.* **43**, 3815–3823 (1972). <https://doi.org/10.1063/1.1661817>
- R.U. Martinelli, M. Ettenberg, Electron transport and emission characteristics of negative electron affinity Al<sub>x</sub>Ga<sub>1-x</sub>As alloys (0 ≤ x ≤ 0.3). *J. Appl. Phys.* **45**, 3896–3898 (1974). <https://doi.org/10.1063/1.1663882>
- W.F. Krolkowski, W.E. Spicer, Photoemission studies of the noble metals. I. Copper. *Phys. Rev.* **185**, 882–900 (1969). <https://doi.org/10.1103/PhysRev.185.882>
- Photon Optics, 1th edition, edited by Li G. C, published by National defense industry Press (2010), page 147.



27. D.H. Dowell, F.K. King, R.E. Kirby et al., In situ cleaning of metal cathodes using a hydrogen ion beam. *Phys. Rev. Spec. Top. Accel. Beams*. **9**, 063502 (2006). <https://doi.org/10.1103/PhysRevSTAB.9.063502>
28. S.V. Nayak, N.M. Badiger, Measurement of K-shell photoelectric absorption parameters of Hf, Ta, Au, and Pb by an alternative method using a weak  $\beta$ -particle source. *Phys. Rev. A* **73**(3), 032707–032707 (2006). <https://doi.org/10.1103/PhysRevA.73.032707>
29. K.S. Puttaswamy, R. Gowda, B. Sanjeevaiah, Photoelectric cross sections derived from the total absorption cross sections in the energy range 5–130 keV. *Can. J. Phys.* **57**(1), 92–98 (1979). <https://doi.org/10.1139/p79-011>
30. C.Y. Fong, M.L. Cohen, Energy band structure of copper by the empirical pseudopotential method. *Phys. Rev. Lett.* **24**(7), 306–309 (1969). <https://doi.org/10.1103/PhysRevLett.24.306>
31. E.C. Snow, Self-consistent energy bands of metallic copper by the augmented-plane-wave method. II. *Phys. Rev.* **157**(3), 570–578 (1968). <https://doi.org/10.1103/PhysRev.171.785>
32. R. Shimizu, K. Goto, On the energy distribution of secondary electrons emitted from metals. *J. Surf. Anal.* **15**(2), 186–194 (2008). <https://doi.org/10.1384/jsa.15.186>
33. M.S. Chung, Improved calculations of secondary electron energy distributions of metals. *J. Appl. Phys.* **46**, 465 (1975). <https://doi.org/10.1063/1.321362>
34. A.G. Xie, L. Wang, L.H. Mu, Formula for maximum secondary electron yield from metals. *Surf. Rev. Lett.* **22**, 1550019 (2015). <https://doi.org/10.1142/S0218625X15500195>
35. A.G. Xie, H.S. Uhm, Y.Y. Chen et al., Maximum secondary electron yield and parameters of secondary electron yield of metals. *Surf. Rev. Lett.* **23**, 1650039 (2016). <https://doi.org/10.1142/S0218625X16500396>
36. P.A. Wolff, Theory of secondary electron cascade in metals. *Phys. Rev.* **95**, 56 (1954). <https://doi.org/10.1103/PhysRev.95.56>
37. A.G. Xie, H.J. Dong, Z. Pan, An electron-induced secondary electron model for photoelectric sensitivity and quantum efficiency of metal surfaces. *Results. Phys.* **26**, 104350 (2021). <https://doi.org/10.1016/j.rinp.2021.104350>
38. J.O.D. Williams, J.S. Lapington, S.A. Leach et al., Using quantum entangled photons to measure the absolute photon detection efficiency of a multi-pixel SiPM array. *Nucl. Instrum. Methods Phys. Res. Sect. A* **958**, 8 (2020). <https://doi.org/10.1016/j.nima.2019.05.008>
39. W. Xu, X. Hou, Y. Meng et al., Deciphering charging status, absolute quantum efficiency, and absorption cross section of multicarrier states in single colloidal quantum dots. *Nano. Lett.* **17**, 7487–7493 (2017). <https://doi.org/10.1021/acs.nanolett.7b03399>
40. H.M. Cobb, *Dictionary of Metals*, 1st edn. (ASM international, 2012), pp. 336–340
41. H. Seiler, Secondary electron emission in the scanning electron microscope. *J. Appl. Phys.* **54**, R1 (1983). <https://doi.org/10.1063/1.332840>
42. A.G. Xie, H.Y. Wu, J. Xu, Parameters of the secondary electron yield from metal. *J. Korean. Phys. Soc.* **62**(5), 725–730 (2013). <https://doi.org/10.3938/jkps.62.725>
43. A.G. Xie, K. Zhon, D.L. Zhao et al., Formulae for low-energy secondary electron yield from different kinds of emitters as a function of measurable variables. *Mod. Phys. Lett. B* **31**(10), 1750105 (2017). <https://doi.org/10.1142/S0217984917501056>
44. A.G. Xie, Y.J. Yao, J. Su et al., A universal formula for secondary electron yield from metals. *Nucl. Instrum. Methods. Res. Sect. B* **268**(17–18), 2565–2570 (2010). <https://doi.org/10.1016/j.nimb.2010.06.012>
45. J. Llacer, E.L. Garwin, Electron-phonon interaction in alkali halides. I. The transport of secondary electrons with energies between 0.25 and 7.5eV. *J. Appl. Phys.* **40**, 2766 (1969). <https://doi.org/10.1063/1.1658075>
46. A.G. Xie, H.J. Dong, Z. Pan, Electron-insulator interaction and secondary electron yield at any Kelvin temperature. *Results. Phys.* **28**, 104554 (2021). <https://doi.org/10.1016/j.rinp.2021.104554>

Springer Nature or its licensor holds exclusive rights to this article under a publishing agreement with the author(s) or other rightsholder(s); author self-archiving of the accepted manuscript version of this article is solely governed by the terms of such publishing agreement and applicable law.